ARPA ORDER 3386

INTERNAL WAVE MEASUREMENT

FINAL REPORT ON OPTICAL VORTICITY METER TASK FOR FUNDED EXTENSION OF CONTRACT NO. N00140-77-C-6670

by

W. T. Mayo, Jr.

5 May 1978

SDL No. 78-6308

Prepared for:

NAVAL UNDERWATER SYSTEMS CENTER
New London, Connecticut 06320

SPECTRON DEVELOPMENT LABORATORIES INC.

ARPA ORDER 3386
INTERNAL WAVE MEASUREMENT

FINAL REPORT ON OPTICAL VORTICITY METER TASK
FOR FUNDED EXTENSION OF
CONTRACT NO. N00140-77-C-6670

by
W. T. Mayo, Jr.

5 May 1978

SDL No. 78-6308

Prepared for:

NAVAL UNDERWATER SYSTEMS CENTER
New London, Connecticut 06320

SPECTRON DEVELOPMENT LABORATORIES INC.

3303 Harbor Boulevard, Suite G-3
Costa Mesa, California 92626 (714) 549-8477

TABLE OF CONTENTS

1.0 INTRODUCTION

1.1 Objective

The purpose of this brief study was to ascertain the conceptual feasibility of the development of a laser optical vorticity meter (LOVM) based on a laser ring interferometer. We postulated that this might be possible if the detection of phase shifts produced by Fizeau drag could be enhanced by the use of multiple beam interferometry techniques. The objective sensitivity is 5 mr/s vorticity with one second averaging time.

1.2 Scope

Our effort under this task has consisted of scientific brainstorming, literature review, analysis, and documentation. Section 2.0 of this report presents a few relevant historical equations and selected results of our literature search. Selected papers are reproduced in the appendices for the convenience of the reader. Section 3.0 describes two postulated LOVM systems and presents a brief sensitivity analysis. Section 4.0 concludes that experimental development of these concepts is not justified at the present. Current efforts in enhancement of fiber ring interferometer sensitivity should be watched closely, and reference beam laser velocimeter techniques should be reexamined.

2.0 BACKGROUND

There are four relevant concepts which are well documented in the literature of physics and engineering which are of interest here. These are: the Fizeau drag effect; the Sagnac effect; the relationship of these effects to ring lasers; the relationship of Sagnac effects to multiple-path passive ring interferometers. A concept which does not appear to have been treated is the relationship of Fizeau drag effects to multiple-path passive ring interferometers with a lossy medium. The first four concepts are documented briefly below and in the references[1-7]. Several of the references are reproduced in the appendices of this report for the convenience of the reader. The last concept is treated in Section 3.0 of this report.

2.1 Sagnac Effect

A simplified schematic diagram of a Sagnac interferometer experiment is illustrated in Figure 1. A laser beam is split into two beams by a beam splitter (BS) which follow the same path C in opposite directions around the circuit composed of the mirrors M_a, M_b, and M_c and BS. The output of the beam splitter to the detector is an interference pattern which is not sensitive to path length variations due to density fluctuations in the propagation medium, vibriations of the mirrors, or other isotropic path length fluctuations. The phase of the output interference pattern is affected by anisotropic propagation

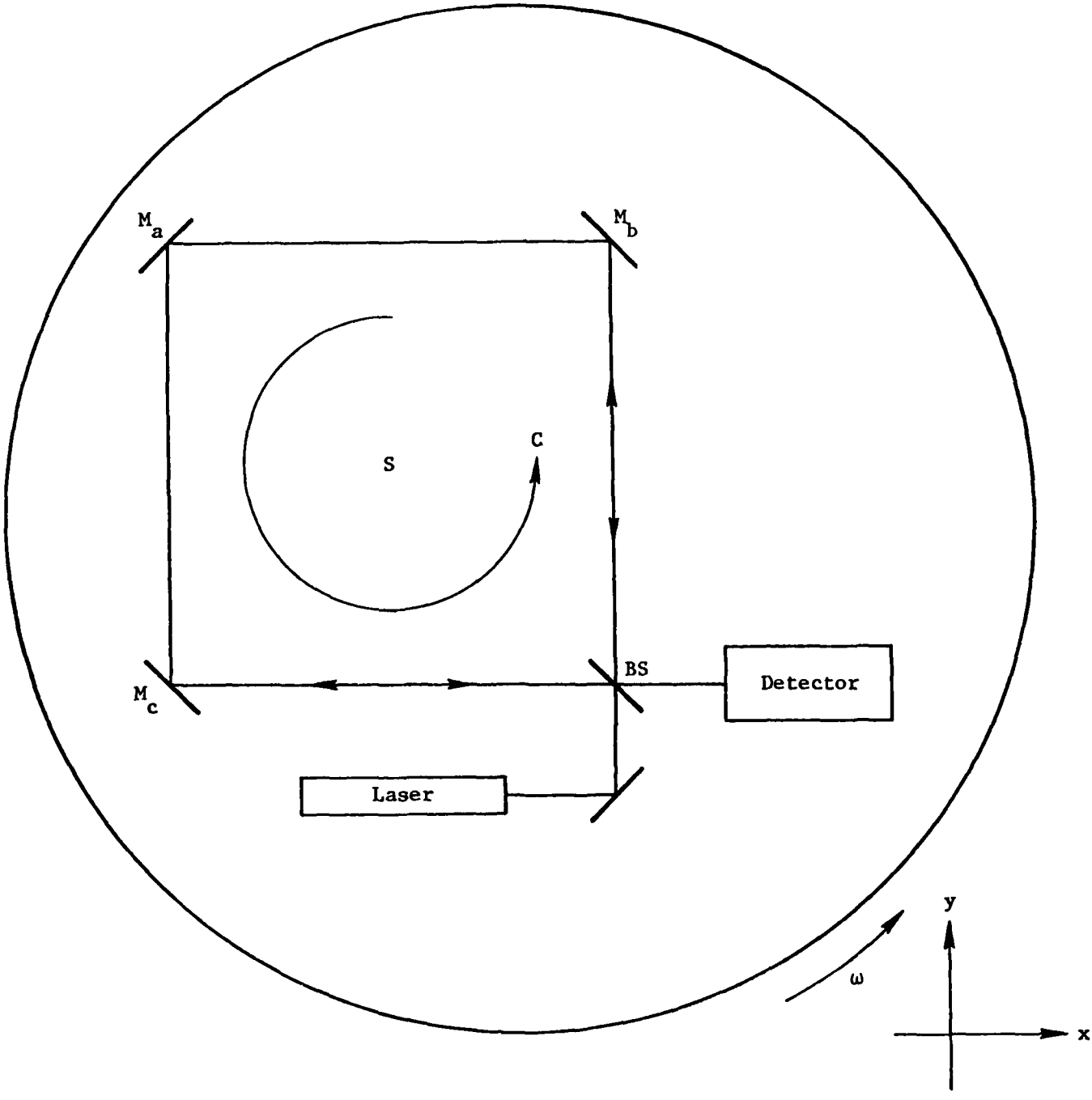

Figure 1. A Simplified Laser Sagnac Interferometer.

effects such as birefringence. The Sagnac effect is an anisotropic effect by which the effective propagation path lengths are changed relative to one another by absolute rotation of the interferometer system about the axis normal to the plane of propagation.

A thorough historical review, along with modern theoretical deviations of the Sagnac effect has been written by Post[1]. This classic paper is reproduced in Appendix A. We may summarize the results, which have been adequately demonstrated experimentally, that when the propagation medium is stationary with respect to the rotating interferometer system, then

$$\Delta z = \frac{4}{c\lambda_o} \bar{\omega} \cdot \bar{S} \tag{1}$$

where Δz = fringe shift expressed in cycles. (2)

$\bar{\omega}$ = vector angular velocity of absolute rotation of the system expressed in radians/second.

c = free-space propagation velocity of light.

λ_o = free-space wavelength of light.

$\bar{S}$ = vector area $S\bar{a}_s$ where S is the area enclosed by the propagation path C, and $\bar{a}_s$ is the unit vector normal to the plane of propagation.

Formula (1) neglects higher order relativistic effects which are subject to some debate but which are negligible in comparison to unity as $\omega^2 S/\pi c^2$. Also *it is important to note Formula (1) is valid even when the propagation path is in a co-moving medium with index of refraction not equal to unity* (see Post, page 476).

In summary, the Sagnac fringe shift is proportional to the absolute rotation rate of the system independent of the index of refraction of a co-moving propagation medium.

2.2 Fizeau Drag

Figure 2 illustrates a typical experiment to measure the change in effective optical propagation velocity or path length which results from uniform linear motion of the liquid propagation medium at velocity V. The light velocities for the two directions of propagation in the moving medium are given by* the Lorentz formula (neglecting an insignificant dispersion term) as

$$u_{\pm} = \frac{c}{n} \pm V\alpha \tag{3}$$

where (4)

$u_{\pm}$ = propagation velocity with or against the velocity V of the moving medium.

c = free-space propagation velocity.

n = index of refraction of moving medium (the remainder of the path is assumed to have n = 1.0).

α = the Fresnel-Fizeau drag coefficient = $1 - 1/n^2$.

The fringe shift, expressed in cycles, is $\Delta tc/\lambda_o$, where Δt is the propagation delay time difference for the path of length L given by

---

* See Page 1148 of Rosenthal[2]. This reference is reproduced as Appendix B.

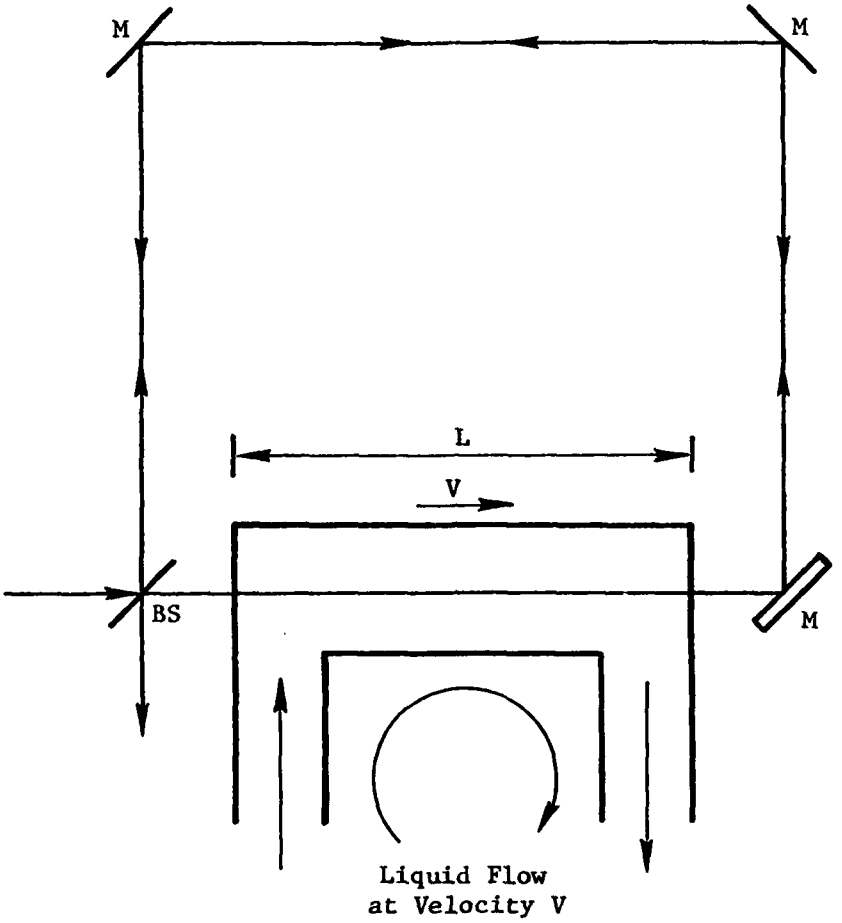

Figure 2. Simplified Fizeau Drag Experiment.

$$\Delta t = \frac{L}{\left(\frac{c}{n} - \alpha V\right)} - \frac{L}{\left(\frac{c}{n} + \alpha V\right)} = \frac{2\alpha VL}{\left(\frac{c^2}{n^2} - V^2\alpha^2\right)} \quad . \tag{5}$$

Thus the fringe shift is given for velocities of the medium small compared with the speed of light by

$$\Delta z = \frac{2\alpha VLn^2}{c\lambda_o} \quad . \tag{6}$$

Now if we allow the Sagnac interferometer of Figure 1 to be placed at rest in a moving medium with nonunity index of refraction n, we may express the Fizeau drag formula in vector line integral form as

$$\Delta z = \frac{2}{c\lambda_o} \oint_C n^2 \alpha \bar{V} \cdot \underline{dl} \tag{7}$$

where the quantities n^2 and α are included under the integral sign because they may be a function of position. Although Post* derives Equation (7) in general, he points out that the value of α as $(1 - 1/n^2)$ has only been verified experimentally for fluids in uniform linear motion. We have no reason to suspect that Equation (7) is not valid for all situations, and will henceforth assume that the Fizeau-Fresnel drag coefficient applies differentially to accelerated fluid flows.

2.3 Ring Laser Gyroscopes

The Sagnac effect describes the apparent shortening of one path with respect to the oppositely directed path around a rotating ring

---

* See Appendix A, Page 484.

interferometer. Rosenthal[2]* pointed out that if a ring laser were constructed, the difference in effective cavity length for the oppositely directed beams would produce a difference in the laser oscillation frequencies whose difference could be detected and used to construct a very sensitive gyroscope. Howard Greenstein[3] recently reviewed the 15 years of laser gyroscope work which has proceeded**. For a ring laser gyroscope, the cavity length induced frequency difference obeys the formula (excluding non-linear lock-in effects):

$$\Delta f = \frac{4\,\bar{\omega} \cdot \bar{S}}{P\,\lambda_o} \tag{8}$$

where Δf is expressed in hertz, P is the length of the perimeter of the enclosed area S_1 and the other quantities are as in Equations 1 and 2 above. This amounts to approximately 1 Hz output frequency for a 1 deg/hr rotation rate with λ = 632.8 nm which would be added to any Fizeau drag effects if the body rotated. There are lock-in effects which typically limit the minimum rotation rate to hundreds of degrees per hour unless bias techniques are used, but even this is quite sensitive.

The ring laser has been used to perform Fizeau drag experiments and is very sensitive to small flow velocities. However, it is clear at the outset that such an approach cannot be used to measure a closed line integral of velocity of a medium unless the

---

* See Appendix B.
** See Appendix C.

flowing medium being measured is also the laser gain medium. Thus, ring lasers cannot be used directly for detection of fluid vorticity.

There are serious problems with ring lasers which are inspiring the development of passive Sagnac interferometers for the optical gyroscope application[3]. However, a ring laser gyroscope could still be a candidate for real time determination of absolute rotation of a vorticity meter stable platform. Some such gyroscopic signal would be required for subtraction from the combined rotation/Fizeau drag signal which would result from the LOVM sensor.

2.4 Laser Ring Interferometer Gyroscopes

The excitement over ring laser gyroscopes was due primarily to promises of large angular sensitivity which has as yet failed to totally materialize due to low rate lock-in effects and flow effects in the laser gain medium. At least two recent developments have led researchers back to passive ring interferometer techniques. One which is very promising uses a coiled single-mode optical fiber to allow many non-interfering multiple passes around the path C*. Coiled fiber systems with one to four kilometers length are under investigation at the University of Utah[4,5] and other locations. There are few published details because, as Dr. Greenstein[6] puts it, this business is "highly competitive" at the present time. These fiber optic techniques may turn out to be superb for making a gryoscope if small phase angle detection problems are solved. These

---

* See Appendix D.

detection problems are the same ones which limit the Fizeau drag concept we will discuss below.

There is another new approach to laser gyroscopes which appears relevant. Ezekiel and Balsamo[7] at MIT* are developing a multiple path interferometer technique, again inspired by Rosenthal, which has sensitivity similar to that of a ring laser but without the disadvantages of having the gain medium in the cavity. In telephone communication with Ezekiel by W. T. Mayo he indicated (February 1978) that he had not thought of using the technique for fluid vorticity measurement but that it might be possible. He further indicated that the primary difficulties would be loss of cavity Q by the presence of the fluid and vibration misalignment of the cavity. These problems are discussed further in Section 3.0 below. In addition, Dr. Greenstein has written a pertinent letter which is reproduced in Appendix F.

---

* See Appendix E.

3.0 MULTIPATH FIZEAU DRAG SYSTEM

This section postulates and briefly analyzes the sensitivity of two Fizeau-drag systems. We begin with a single-pass Sagnac interferometer system and then consider multipath sensitivity enhancement techniques.

3.1 Multiple Circuit Interferometers

Let us assume that the system shown in conceptually in Figure 1 is stationary in an absolute rotational sense with the three labeled mirrors and the beam splitter all immersed in a liquid of index of refraction n which is flowing with vector velocity field $\bar{V}(r)$. The phase shift due to Fizeau drag is expressed by Equation 7 above. By using Stokes curl theorem we may express Equation 7 alternately as

$$\Delta z = \frac{2}{c\lambda_o} \iint_A n^2\alpha(\nabla x\bar{V}) \cdot \underline{dA} = \frac{2}{c\lambda_o} \oint n^2\alpha\bar{V} \cdot \underline{dl} \qquad (9)$$

As an example, we evaluate Equation 9 for the case where the system of Figure 1 is one meter on a side, the laser wavelength is 0.5×10^{-6} m, the medium is water, and the vorticity in velocity produces a difference in the tangential velocity component of 5 mm/sec between each of the two sets of opposite sides of the square interferometer. This corresponds approximately to a point vorticity of 5 mr/s. The result is:

$$\oint_C \bar{V} \cdot dl = 10 \times 10^{-3}\ m^2 s^{-1} \qquad (10)$$

$$\Delta z = 1.025 \times 10^{-4} \text{ cycles.}$$

This amount of shift is difficult to measure, but is within laboratory state-of-the-art.

Consider the degrading effects of incoherent multiple forward scatter by particulates. In very clear water, the attenuation length can approach 20 meters. More typically in clear water, the scattering length is less than 20 meters. The majority of the scattered light does occur in the forward direction over tens of milliradians. If microradian spatial filters were used to remove the majority of the particle scattered light, it would not degrade the detection process with extra photon noise and optical phase noise. It would seem that using such techniques would allow at least one pass around a 4 meter path in most clear waters. Perhaps a multiple path system with two to five passes would be possible. This would bring the required sensitivity to 2-5 x 10^{-4} cycles.

3.2 Ring Fabry Perot Interferometers

The ring Fabry Perot interferometer concepts of Ezekiel and Balsamo* offer a different concept for evaluation. The resonant frequency of the ring cavity is different for the CW and CCW beams due to both the Sagnac effect and the Fizeau drag effect. The

---

* See Appendix E.

difference in cavity resonance peak frequency for the oppositely directed beams would be given by the linear ring laser formula for drag by Equation 56 of Post (see Appendix A, page 484) as

$$\Delta f = \frac{2}{\lambda_o} \frac{\oint_C n^2 \alpha \bar{V} \cdot \underline{dl}}{\oint_C n \, dl} \qquad (11)$$

By comparing this equation with our Equation 9 above, we see that the resonant *frequency* difference is nominally different in magnitude from the *phase* shift of a single pass Sagnac/Fizeau inferferometer by a factor of c divided by the optical path length around the perimeter. For our previous example, this is a factor of $3 \times 10^8/5.32 = 5.639 \times 10^7$ with the result that the 1 mm/sec/meter shear would produce a resonant cavity frequency difference of 578 Hz.

Now it would seem that 578 Hz might be a detectable frequency shift. This would easily be the case if we were dealing with the difference between two monochromatic oscillators separated in frequency by this amount. Unfortunately in the passive ring Fabry Perot systems such as Ezekiel and Balsamo, one must sense the location of the center frequency of resonance of the cavity under conditions where the cavity oscillation frequency characteristic is quite broad. According to Dr. Greenstein (see Appendix F) the cavity width is typically a few Megahertz for a nearly lossless cavity.

The effect of a laser (or any etalon) cavity with high Q is achieved by an equivalent of many transits of a photon around the path of the cavity. The consequence of scattering losses is to reduce the number of circuits, or cavity Q, and also increase width of the resonant curve for the cavity. Considering the losses in seawater, the cavity Q would be more on the order of 2 than greater than 99 if a square circuit one meter on a side were used. In addition, Dr. Ezekiel points out that the two laser beams must be injected into the passive ring cavity with tight tolerances on alignment, which would be difficult to achieve in the ocean environment.

4.0 DISCUSSION

There are many reasons not to put a laser cavity totally into seawater. Even if the extinction losses did not hopelessly spoil the cavity Q, the problem of keeping the mirrors clean to laser cavity specifications would be difficult, if not impossible. We do not now see how a practical adaptation of the Ezekiel and Balsamo techniques can be made.

The fundamental limitations of the passive ring interferometer technique will ultimately depend on photon noise limits, particle multiple scattering, and refractive propagation effects. Photon noise is not an issue for the present objectives, providing that fringe visibility is not destroyed by multiple scattering.

The technological question for the passive ring interferometer which is immediately apparent is how to measure a phase shift of 1 in 10^4 cycles. Carefully performed laboratory measurements have exceeded one part in 10^6 for small sinusoidal vibrational displacements of phase[8]. The techniques used are not applicable to absolute DC phase measurements. Victor Vali and Richard Shorthill of the University of Utah are faced with the exact same problem for enhancing the sensitivity of the fiber ring gyro. Dr. Shorthill has indicated by telephone that they are investigating both heterodyne techniques and techniques which would utilize microprocessor curve fitting of linear detector array outputs. He feels that the

attainment of $1:10^4$ or better is not unreasonable for the future. Thus, it would seem appropriate to watch developments in the fiber ring gyro research arena and to determine what classified results may be available, if any, from defense contractors.

The consensus of opinion in September 1976 was that fringe velocimetry has shown itself to be superior in signal-to-noise ratio over reference beam or heterodyne LV systems. This conclusion has been developed in the past in flow tunnel situations where transverse velocity components were to be measured. If one considers measuring axial velocity components, the frequency sensitivity of a backscatter reference beam system is much larger and transit time broadening effects are reduced. This, in turn, allows increasing the transmitter beam diameter and the receiver beam diameter and thus increasing both the incident power density in the probe volume and the receiver collection area.

Now, if we consider probe beams directed in the direction of the mean flow, the transit time broadening effects are greatly reduced due to the fact that the length greatly exceeds the width. This geometry would be totally useless in a wind tunnel for obvious reasons. Also, for all but very slow wind tunnel velocities, the 4 MHz/m/sec shifts are too large to handle electrically. Thus, no one with a lot of LDV experience ever considered a "head-on" backscatter reference beam system.

William Stachnik, NUSC, has suggested a differential heterodyne optical system which removes the mean velocity shift due to translation *optically* so that large electronic dynamic range would be avoided. When this idea is combined with the above concepts, we see that a new kind of heterodyne system has been conceived. These ideas have been extended to include the possibility of a compact arrangement which measures two orthogonal components of shear in the horizontal plane. Mr. Stachnik has documented these ideas in a memo which we reproduce in Appendix G.

5.0 CONCLUSIONS

The Fizeau drag effect produces a very small anisotropic modification of effective propagation time for oppositely circulating monochromatic beams of light in a ring interferometer structure.

The effect may be observed either as a phase shift between counter rotating beams derived from the same laser or as a shift of the peak resonant frequency of the ring structure taken as a passive laser cavity.

We have considered experimental optical configurations of reasonable dimensions (1 m/square) and found them to be inadequate in sensitivity for detection of small vorticity (5 mr/s) for even the clearest ocean water unless electronic phase detection art is developed. However, such developments are expected to occur under current fiber optic laser gyro research programs.

There are new possibilities for development of a laser velocimeter shear meter which arise out of recent ideas for differential heterodyne detection schemes which cancel translational velocities prior to electronic processing.

We recommend further funding concerning laser velocimeter techniques and careful "wait and see" monitoring of present laser (fiber/ring) gyro research in small phase detection.

6.0 REFERENCES

1. E. J. Post, "Sagnac Effect", Reviews of Modern Physics, 39, 475-493, (April 1967).

2. A. H. Rosenthal, "Regenerative Circulatory Multiple-Beam Interferometry for the Study of Light-Propagation Effects", J. Optical Society of America, 52, 1143-1148, (October 1962).

3. H. Greenstein, "Progress on Laser Gyros Stimulates New Interest", Laser Focus, p. 60, (February 1978).

4. V. Vali and R. W. Shorthill, "Fiber Ring Interferometer", Applied Optics, 15, 1099-1100, (May 1977).

5. S. Balsamo, S. Ezekiel and V. Vali, Letters to "Reader's Column", Laser Focus, p. 8, (November 1975).

6. H. Greenstein, Personal Communication.

7. S. Ezekiel and S. R. Balsamo, "Passive Ring Resonator Laser Gyroscope", Applied Physics Letters, 30, 478-480, (May 1977).

8. G. E. Moss, L. R. Miller, and R. L. Forward, "Photon-Noise-Limited Laser Transducer for Gravitational Antenna," Applied Optics, Vol. 10, p. 2495 (November 1971).

REVIEWS OF MODERN PHYSICS VOLUME 39, NUMBER 2 APRIL 1967

Sagnac Effect

E. J. POST
Air Force Cambridge Research Laboratories, Bedford, Massachusetts

A revived interest in the Sagnac effect has recently resulted from the development of the self-oscillating laser version of the original Sagnac interferometer. The Sagnac interferometer or ring laser is an example of an electromagnetic sensor of absolute rotation, so historical and theoretical background information is useful in evaluating the possibilities of electromagnetic sensing of absolute rotation. A critical literature study of the many experimental ramifications and the older kinematical theory of the effect is presented. This geometric optical theory is then complemented and compared with more recent work that is based on a physical optical analysis using a complete electromagnetic description of the phenomenon.

CONTENTS

I. ABSOLUTE MOTION VERSUS RELATIVE MOTION

An observer enclosed in a "black box" has no way of telling whether his box is in uniform translational motion. A state of uniform translational motion can be established only by visual observation of the change of position of the box with respect to other objects. This requires that the observer extend his observation outside the black box. We define the "black box" as an enclosure which does not permit physical observations outside itself. Observations made inside the enclosure are called "intrinsic." There are no intrinsic physical means, either mechanical or optical, of detecting a state of uniform motion of the box.

The physical equivalence of all uniform translatory motions establishes a set of equivalent space–time frames of reference known as inertial frames. These are in relative motion with respect to each other and are mutually related by Lorentz transformations. Conversely the Lorentz group determines the set of all inertial frames. The Lorentz group thus expresses a space–time symmetry: free space exhibits the same physical properties with respect to all inertial frames. The space–time symmetry defined by the Lorentz group is comparable with the crystal symmetry defined by the crystallographic groups except that the crystal groups are discrete and represent purely spatial symmetries. The physical properties of a crystal appear the same with respect to the discrete set of frames permitted by its crystal symmetry group (Neumann principle). Analogously free space appears the same with respect to the continuous set of inertial frames related by the Lorentz group.

Any frame of reference that is not an inertial frame is in some way an "accelerated" frame. The acceleration is observable inside the box as a mechanical force field. The presence and the nature of a mechanical force field inside the box enable us to establish in what respect the space–time frame of the box deviates from an inertial frame, without observation of external objects.

The force field in the box can be of a gravitational or of a "kinematical" origin. It is, in principle, possible to distinguish between the two force fields by intrinsic means. A box at rest on the surface of a stationary (nonrotating) earth is subject to a purely gravitational field, the force lines converging towards the center of the earth. A box on the periphery of a rotating disk also exhibits an internal force field the lines of which diverge from the axis of rotation. An observer moving inside the box that is on a rotating disk is in addition subject to a Coriolis force. The Coriolis force is absent in the case of a purely gravitational force field. A linearly accelerated motion does not give rise to a Coriolis force. Its lines of force converge to a point at infinity instead of towards a finite point as would be the case for a gravitational source.

Thus the nature of the acceleration at a point inside the box can be established by exploring the neighborhood of that point. Fock calls this the distinguishability in "the large" of acceleration and gravitation [Fock (1959), p. 208]. A state of kinematical acceleration is thus associated with a state of absolute motion with respect to all inertial frames.

Very sensitive devices have been developed for measuring acceleration fields mechanically. The pendulum is used to measure the earth's gravitation; the Foucault pendulum can be used to measure the earth's rate of rotation. Linear accelerations can be measured by a differential frequency shift of loaded vibrating

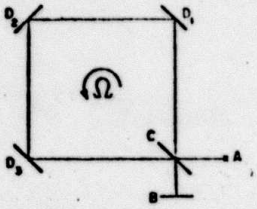

FIG. 1. Schematic of Sagnac's interferometer. A=light source; B=observer; C=beam splitter (half-silvered mirror); D_1, D_2, and D_3 are corner mirrors.

strings. The gyroscope is one of the most sensitive devices that responds even to the slightest deviation of its frame from an inertial frame. This direction preserving property of the gyroscope is widely used in navigation.

The mechanical means for measuring accelerations have been so good that comparatively little attention has been given to optical or, in general, to electromagnetic means. If inertial frames are not intrinsically distinguishable, either by mechanical or by optical means, and if noninertial frames are intrinsically distinguishable by mechanical means, then one can expect, on the basis of electromechanical parallelism, noninertial frames also to be distinguishable by means of purely electromagnetic methods. (Mechanical methods utilizing optical and electrical means for increasing the read-out sensitivity are obviously to be classified as mechanical methods of acceleration detection.)

Sagnac (1913) first demonstrated the feasibility of an optical experiment capable of indicating the state of rotation of the frame of reference in which his interferometer was at rest. The red shift of spectral lines is another but much less sensitive example of intrinsic detection of acceleration. Some little known unipolar induction phenomena share with the Sagnac effect the basic feature of an intrinsic detection of rotation. The emphasis in the following is on the Sagnac effect.

II. SAGNAC-TYPE EXPERIMENTATION

Earlier review of the Sagnac effect and its experimental and theoretical ramifications have been given by von Laue (1920), Metz (1952), and by Zernike (1947). The geometric optical nature of these experiments permits a simple kinematical analysis which was succinctly treated by Zernike.

The basic principle of Sagnac's interferometer is given in Fig. 1. The light beam coming from the source A is split by C into a beam circulating the loop in a clockwise direction $CD_3D_2D_1C$ and a beam circulating the same loop in a counterclockwise direction $CD_1D_2D_3C$. The two beams are reunited at C so that interference fringes are observed in B. When the whole interferometer with light source and fringe detector is set in rotation with an angular rate of Ω rad/sec, a fringe shift ΔZ with respect to the fringe position for the stationary interferometer is observed, which is given by the formula

$$\Delta Z = 4\Omega \cdot A/\lambda_0 c, \qquad (1)$$

in which A is the area enclosed by the light path. The vacuum wavelength is λ_0 and the free-space velocity of light is c. The scalar product $\Omega \cdot A$ denotes that ΔZ is proportional to the cosine of the angle between the axis of rotation and the normal to the optical circuit.

For a proper execution of the Sagnac experiment it is mandatory that the mirror positions do not change under the influence of centrifugal force. Pattern changes due to distortion of the interferometer would not in general result in a pure fringe shift and are therefore distinguishable from the expected effect. Another criterion is that distortions do not depend on the direction of rotation.

The fringe shift given by formula (1) can be doubled by making a comparison between the fringe positions obtained on rotating in opposite directions. Sagnac (1914) thus obtained, for the wavelength of indigo mercury light and a loop area $A=866$ cm², a fringe shift of 0.07 fringes for a rate of rotation of 2 rps. This fringe shift, he writes, was clearly detectable.

The fringe shift detectability at that time was probably of the order of 0.01 of a fringe. The precision of Sagnac's experiment therefore may have been close to marginal. Figure 2 gives an impression of Sagnac's original equipment. The light source and the fringe (shift) detection occur on the rotating disk. Sagnac also established that the effect does not depend on the shape of the loop or the center of rotation.

A German graduate student, Harress (1911), performed a very similar experiment for a thesis project a few years before Sagnac did his experiment. Harress

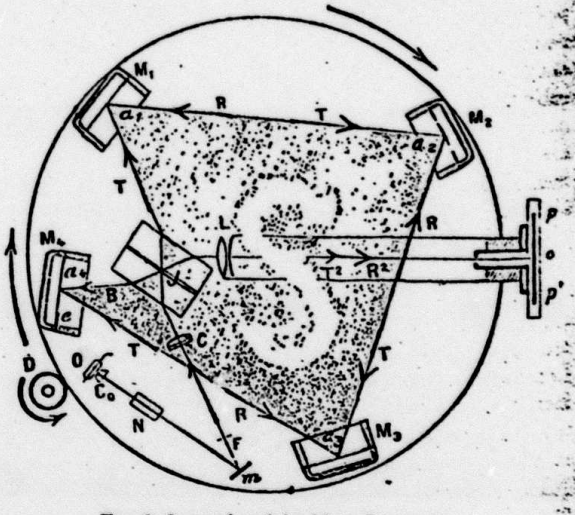

FIG. 2. Sagnac's original interferometer.

used an optical circuit which consisted of a ring of totally reflecting prisms, shown in Fig. 3. The light was propagated in the glass.

Harress' objective was quite different from Sagnac's. Harress wanted to measure the dispersion properties of glasses [Michelson (1886) and Zeeman (1919)] and he felt that a ring interferometer would be a suitable instrument. [Harress' thesis is not available in this country. The above information was extracted from the subsequent discussions of Harress' experiment by Harzer (1914) and von Laue (1920).] The motivation for choosing this arrangement was perhaps based on the idea that it is technically advantageous to substitute a circular motion for the linear motion encountered in the Fresnel-Fizeau experiment for the dragging of light in a moving optical medium.

The Fresnel-Fizeau coefficient of drag α is given by the expression

$$\alpha=(1-n^{-2}-\partial \ln n/\partial \ln \lambda). \qquad (2)$$

Harress apparently assumed that the fringe shift that is observed by rotating the interferometer is due solely to the "dragging" of the light by the moving glass medium. The effect would vanish when expression (2) vanishes, which is the case for free space $n=1$.

By substituting a circular motion for a linear motion Harress tacitly assumed the absence of exactly the effect that Sagnac was looking for. The dispersion data obtained by Harress did not agree well with data available from other methods. Harress did not live to work further towards the solution of this discrepancy.

Harzer (1914) reworked Harress' data on the basis of a different kinematical theory which properly accounted for the rotation. He found in the same year and presumably independently of Sagnac that there would also be a free-space effect of the magnitude given by (1). In addition he came to the interesting conclusion that formula (1), as is, remains valid whether or not a comoving refracting medium is placed in the path of

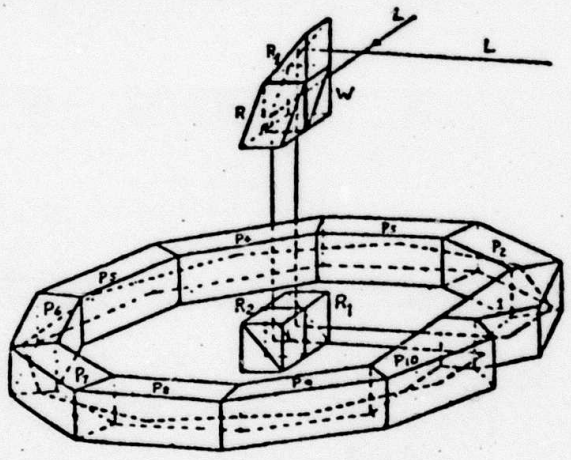

FIG. 3. Harress' ring interferometer.

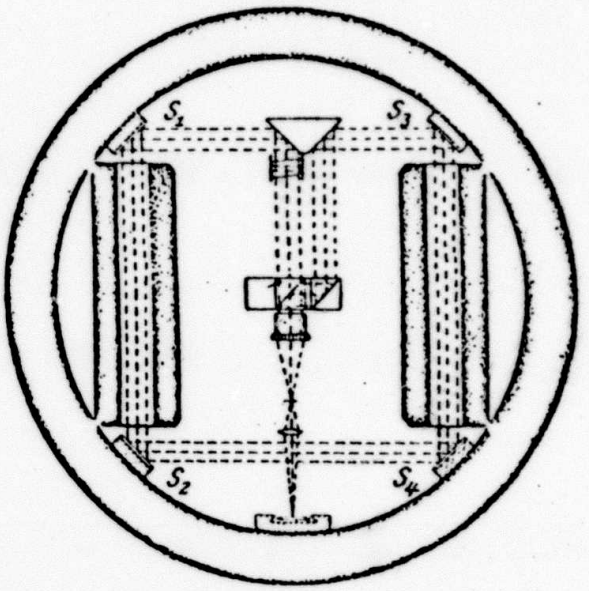

FIG. 4. Interferometer used in Pogany's second experiment with two glass rods in the light path.

the light beam. Hence the fringe shift ΔZ is solely determined by the free-space wavelength λ_0 and the free-space velocity c; a result not suggested by the structure of formula (1) because the product of wavelength and propagation velocity in the medium is proportional to $1/n^2$.

Harzer (1914) expressed surprise that Harress' reworked data also suggested that the dispersion term $\partial \ln n/\partial \ln \lambda$ has no influence on the final fringe shift. It would not have been possible to draw this conclusion if Harress' data had not been considerably more precise than Sagnac's.

Einstein (1914) subsequently pointed out in a short note that the dispersion term in (2) really stems from a Doppler shift due to a motion between source and medium. Inspection of Fig. 3 shows that there is no indication for introducing this correction in connection with the Harress' ring interferometer.

A Sagnac experiment of great precision was subsequently performed by Pogany (1926). With a loop area $A=1178$ cm^2, $\Omega=157.43$ rad/sec, and $\lambda_0=5460\times10^{-8}$ cm, he reproduced within 2% the theoretically expected (double) fringe shift $\Delta Z=0.906$.

Two years later he repeated the experiment, this time with two glass rods in the path of the light beam. He came within 1% of the theoretically expected fringe shift. The experimental arrangement for Pogany's second experiment (1928) with the glass rods in the light beam is shown in Fig. 4. The ruggedness of the construction is demonstrated by the fact that he could still observe fringes at 3000 rpm.

Michelson and Gale (1925) succeeded in demonstrating the rotation of the earth by means of the

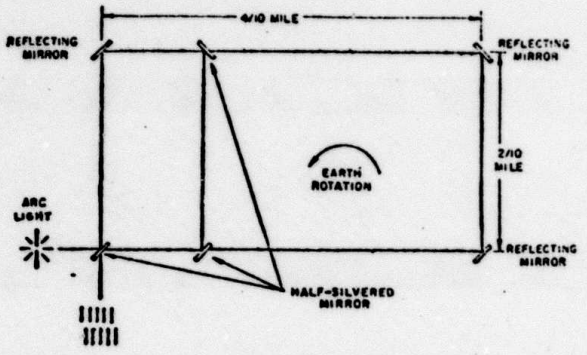

FIG. 5. Michelson–Gale interferometer with calibration circuit.

Sagnac effect. To obtain the required sensitivity they had to choose an unusually large size for the surface area enclosed by the beam (Fig. 5).

In this case the fringe shift had to be shown by changing the surface area A of the loop, instead of the rate of rotation Ω. Because of the calibration circuit and the fact that it was necessary to have the light beam travelling in vacuum to prevent blurring by unwanted Fresnel–Fizeau drag phenomena, the Michelson–Gale experiment was a major optical achievement.

Michelson (1897), prior to Sagnac (1914) and Harress (1911), attempted a similar experiment, although instead of independently rotating the interferometer he hoped to obtain an indication of the rotational motion of the earth with respect to the ether. The results were inconclusive. He also obtained a relation of the form (1) except for a calculational error of a factor of 2, which was corrected in the later paper on the successful experiment with Gale (1925). Apparently Michelson never placed a (smaller loop) interferometer on a uniformly rotating turntable.

To avoid possible confusion, it may be remarked that the beam path in the more well-known Michelson–Morley (1886) interferometer, which *was* mounted on a turntable, does not enclose a finite surface area; therefore no fringe shift can be expected as a result of a uniform rotation of the latter.

Summarizing, the experiments of Sagnac, Pogany, and Michelson–Gale and the results of Harress, as reinterpreted by Harzer, demonstrate beyond doubt the following features of the Sagnac effect. The observed fringe shift

(a) obeys formula (1); $\Delta Z = 4\vec{\Omega}\cdot\vec{A}/\lambda_0 c$

(b) does not depend on the shape of surface area A;

(c) does not depend on the location of the center of rotation;

(d) does not depend on the presence of a comoving refracting medium in the path of the beam.

Dufour and Prunier (1937) confirmed that the fringe shift does not depend on whether the observations are made on the rotating system. Depending on the experimental arrangement, one would expect a slight shift due to a possible Doppler shift in wavelength between a stationary point of observation and the point on the disk where clockwise and counterclockwise beams reemerge reunited (the beam splitter). If v is the mutual velocity of stationary observer and beam splitter, the difference would be

$$\delta(\Delta Z) = \frac{4A\Omega}{c\lambda_0(1+v/c)} - \frac{4A\Omega}{c\lambda_0} \approx -(4A\Omega/c\lambda_0)(v/c), \tag{3}$$

which is v/c times smaller than the effects one wants to observe.

A similar argument holds when one uses a stationary instead of a comoving light source.

Dufour and Prunier (1942) also did an experiment whereby the light traverses a stationary optical medium while the interferometer is rotating. Their experiment indicated that the observed fringe shift increases with the presence of a stationary medium in the beam. The effect of the medium vanishes only if the medium rotates with the interferometer.

Invention of the laser has opened new horizons in the art of interferometry. The measurement of optical beat frequencies, as an alternative to fringe shift measurements, has become a realistic possibility. A self-oscillating version of the Sagnac ring was suggested by Rosenthal (1962) and was subsequently brought into operation by Macek and Davis (1963). This ring laser lends itself almost ideally to generating an unusually stable beat between two optical frequencies, because the clockwise and counterclockwise modes occur in the same optical cavity. Although the individual modes may fluctuate many MHz due to the ever-present mechanical instabilities, the frequency difference can nevertheless be stable to within a few Hz because the two modes have almost identical fluctuation.

The enantiomorphic symmetry of the two modes makes them prone to locking as soon as slight nonlinearities occur in the laser medium. Hence the symmetry that enhances the beat frequency stability also invites a new complication which can be overcome only by artifically introducing an extra asymmetry in the beam path.

A nonreciprocal element, which has a different optical path length for the clockwise and the counterclockwise beams, can be used for the purpose of unlocking. In fact, the Sagnac effect itself is nonreciprocal and can be used by providing an extra mechanical rotation as a bias. A Faraday cell is an electromagnetic equivalent that leads to the same result. The enhanced asymmetry has, however, an adverse effect on the stability of the beat frequency because of the incomplete cancellation of fluctuations.

The ring laser (Fig. 6) is the most recent development in experimental devices based on the Sagnac effect. This instrument also invites modifications similar to those for the ring interferometer. For instance, how does a refracting medium in the path of the beam affect the beat frequency for a given rate of rotation? There is as yet no published material pertaining to such experiments.

In Sec. IV it is shown that, unlike the corresponding result for the ring interferometer, a comoving optical medium in the laser beam affects the beat frequency.

III. GENERAL ASPECTS OF THE THEORY

The following sections compare the results of the kinematical analysis of the Sagnac effect with the asymptotic results of an electromagnetic discussion of the Sagnac effect. The required agreement between these different approaches provides valuable information concerning the electrodynamics of accelerated systems.

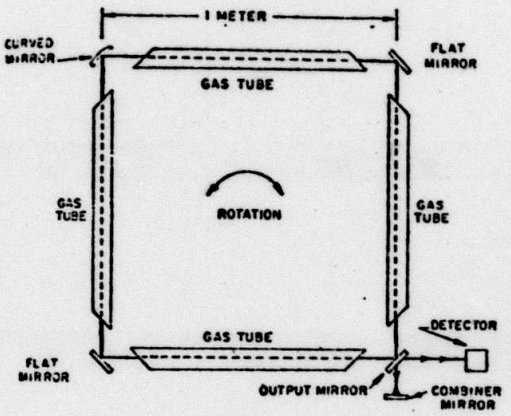

FIG. 6. The ring laser (Macek and Davis, 1963).

The kinematical and the electromagnetic approaches each permits discussion from the point of view of the stationary observer and discussion from the point of view of the comoving observer. The nature of the Sagnac experiment requires, as mentioned in the previous section, a first order agreement between these two possibilities of observation. The organizational diagram, shown in Fig. 7, gives a general view of the mutual relations of these different methods of analyzing the problem.

The analyses corresponding to the possibilities indicated in Fig. 7, require that observations made by the stationary observer can be related to observations made by the comoving observer. The mathematical interconnection of these different points of view requires knowledge of a coordinate transformation which provides a physically meaningful interrelation within the frame of the principle of general space–time covariance.

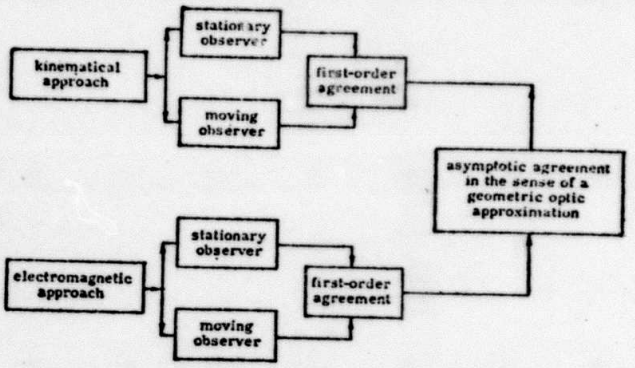

FIG. 7. Flow diagram for methods of analysis.

For uniform rotation in the case of the Sagnac effect one would expect on intuitive grounds that a Galilean rotation (absolute time) might give the correct choice of space–time coordinate transformation. In consideration, however, of well-known experiences with electromagnetic theory in the realm of uniform translations where the Galilei translation (absolute time) is not an adequate substitute for a Lorentz translation, it is useful to give special attention to the question of selecting the right transformation for uniform rotations.

The problem can be suitably analyzed for the following simple but physically conceivable configuration. Suppose the light beams are constrained to follow a circular path of radius R as illustrated in Fig. 8. We calculate the time difference between a counterclockwise circulation (a) and a clockwise circulation (b) of the light as seen by a stationary observer. The two beams leave the beam splitter when it is in position C. The counterclockwise circulation is opposite to the direction of rotation and meets the beam splitter again in the new position C′ shifted by $\Delta s'$ with respect to C. The clockwise beam, travelling in the same direction as the direction of rotation, meets the beam splitter in the later position C″, shifted by $\Delta s''$ with respect to C. The geometry of Fig. 8 gives the following relations, in which c is the free-space light velocity in an inertial frame and Ω the rate of rotation of the circular inter-

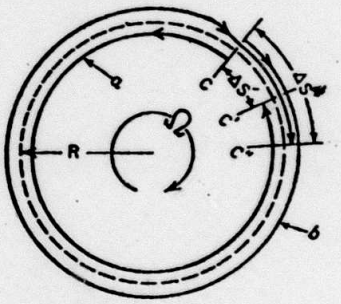

FIG. 8. Simplified Sagnac configuration.

ferometer:

$$\tau' = (2\pi R - \Delta s')/c = \Delta s'/\Omega R, \tag{4}$$

$$\tau'' = (2\pi R + \Delta s'')/c = \Delta s''/\Omega R. \tag{5}$$

Eliminating $\Delta s'$ and $\Delta s''$ from Eqs. (4) and (5), one obtains for the time difference

$$(\Delta\tau)_s = \tau'' - \tau',$$

$$(\Delta\tau)_s = 4\pi R^2\Omega/[c^2 - (\Omega R)^2], \tag{6}$$

and for $\pi R^2 = A$, the surface area of the circular loop,

$$(\Delta\tau)_s = 4\Omega A/[c^2 - (\Omega R)^2]. \tag{7}$$

The time interval $(\Delta\tau)_s$ between the consecutive positions C′ and C″ of the beam splitter is observed in the stationary frame and is therefore dilated by a factor γ. Hence the time interval $(\Delta\tau)_m$ observed on the moving beam splitter itself would be

$$(\Delta\tau)_m = (\Delta\tau)_s/\gamma, \tag{8}$$

or according to Eq. (7)

$$(\Delta\tau)_m = 4\Omega A/\gamma(c^2 - \Omega^2R^2). \tag{9}$$

Following Langevin (1921), let us now attempt to evaluate $(\Delta\tau)_m$ directly by transforming the line element to a rotating frame of reference. As Langevin (1937) remarked, several transformations lead to the experimentally observable first order result of Eq. (1). This number of possibilities can be restricted to essentially one transformation by demanding consistency with the presumably higher order correct result given by Eq. (9).

The line element in polar coordinates for an inertial frame is given by

$$ds^2 = c^2\,dt^2 - dr^2 - r^2\,d\phi^2. \tag{10}$$

The transformation

$$dt = \gamma\,dt',$$

$$dr = dr',$$

$$d\phi = d\phi' + \gamma\Omega\,dt', \tag{11}$$

converts Eq. (10) into the form for the rotating frame,

$$ds^2 = \gamma^2c^2\,dt'^2 - dr'^2 - r^2(d\phi' + \gamma\Omega\,dt')^2, \tag{12}$$

in which γ is an at present undertermined factor in the transformation (11).

The line element vanishes for free-space propagation. The circular symmetric path of the beams occurs at the radius $r' = R$, hence $dr' = 0$, and Eq. (12) becomes

$$ds^2 = \gamma^2c^2\,dt'^2 - R^2(d\phi' + \gamma\Omega\,dt')^2 = 0. \tag{13}$$

Equation (13) is quadratic in the time element dt' and has the roots

$$(dt')_{1,2} = \pm Rd\phi'/(c \mp \Omega R)\gamma, \tag{14}$$

corresponding to clockwise and counterclockwise propagation of the light. The circulation times t_1' and t_2' in the rotating frame are obtained by integrating ϕ' from $0 \to 2\pi$ and $0 \to -2\pi$, respectively,

$$t_1' = 2\pi R/(c - \Omega R)\gamma,$$

$$t_2' = 2\pi R/(c + \Omega R)\gamma, \tag{15}$$

where it is assumed that γ does not depend on the angle ϕ'.

The time difference in the rotating frame then becomes

$$t_1' - t_2' = (\Delta\tau)_m = 4\pi\Omega R^2/\gamma(c^2 - \Omega^2R^2), \tag{16}$$

or for $\pi R^2 = A$,

$$(\Delta\tau)_m = 4A\Omega/\gamma(c^2 - \Omega^2R^2), \tag{17}$$

which is the same as Eq. (9), obtained by applying the time dilation factor γ directly to the time interval for the stationary frame $(\Delta\tau)_s$. Hence the agreement between the results of Eqs. (17) and (9) holds regardless of the value of γ, provided γ is independent of ϕ'.

Langevin took the particular value

$$\gamma = 1, \tag{18}$$

which makes transformation (11) an absolute time Galilean-type rotation

$$d\phi = d\phi' + \Omega\,dt. \tag{19}$$

The calculated value of $\Delta\tau$ is then the same for stationary and for moving observers

$$(\Delta\tau)_m = (\Delta\tau)_s = (4A\Omega/c^2)[1 - (\Omega R/c)^2]^{-1}. \tag{20}$$

If we take, for the time dilation, the well-established expression

$$\gamma = [1 - (\Omega R/c)^2]^{-1/2}, \tag{21}$$

one still has according to Eq. (7)

$$(\Delta\tau)_s = (4A\Omega/c^2)[1 - (\Omega R/c)^2]^{-1}. \tag{22}$$

but for $(\Delta\tau)_m$ one now has

$$(\Delta\tau)_m = (4A\Omega/c^2)[1 - (\Omega R/c)^2]^{-1/2}. \tag{23}$$

Transformation (11) now differs from the familiar Galilean rotation (19). It becomes

$$dt = dt'/[1 - (\Omega R/c)^2]^{1/2},$$

$$dr = dr',$$

$$d\phi = d\phi' + \Omega\,dt'/[1 - (\Omega R/c)^2]^{1/2}. \tag{24}$$

[See the Appendix for an alternate way of obtaining (24).]

The calculated values for $\Delta\tau$, (20), (22), and (23) are not experimentally distinguishable with presently available equipment, because for

$$\Omega R \ll c, \tag{25}$$

corrections in $\Delta\tau$ are of the order

$$(\Omega R/c)^2 \Delta\tau, \tag{26}$$

which is still one order smaller than the Doppler correction (3) which occurs when observing fringe shifts instead of time intervals.

For all practical purposes, one may accept as adequate for the time interval, in the stationary as well as in the rotating frame, the formula

$$\Delta\tau = 4A\Omega/c^2, \tag{27}$$

and for the fringe shift the formula

$$\Delta Z = 4A\Omega/c\lambda_0, \tag{28}$$

which is the same as (1). The latter formula is obtained from (27) by converting the time difference to a fringe shift, by multiplication by c/λ_0.

Langevin (1937), and much later and presumably independently Trocheris (1949), have pointed out that the transformation

$$dt = dt' + (\Omega R^2 d\phi'/c^2) \tag{29}$$

can also be used to obtain an expression for $\Delta\tau$. By integrating $d(t-t')$ over $\pm 2\pi$ for clockwise and counterclockwise beams, respectively, and subsequently subtracting one obtains

$$\Delta\tau = 4\Omega A/c^2. \tag{30}$$

Equation (29) is a recasting of the first-order Lorentz transformation into polar coordinates after which it is applied to the periphery of the circular optical loop. The first order approximation of the Lorentz transformation is required to give t and t' equal time units, which means that $\gamma = 1$.

The physical difference between (24) and (29) is that (29) implies a local time nonuniformity and spatial isotropy versus a nonreciprocal propagation anisotropy resulting from (24). In Sec. V we see that the nonreciprocal features associated with rotating systems support transformations (11) or (24) rather than transformation (29). In the Appendix it is shown why (24) rather than (29) has the proper asymptotic relation to the Lorentz transformation.

We thus conclude that transformation (24) has a unique and preferred status if we concede that the time dilation (21) is a unique and established relation which is also valid beyond the realm of uniform translation. The experimentation that was discussed in the previous section can hardly be expected to establish the magnitude of the higher-order terms, even if considerable refinement in observation were applied to improve the sensitivity. In the following we therefore consider results of first order in Ω only.

The search for a physically meaningful transformation for rotation is not aided in any way whatever by the principle of general space–time covariance, nor is it true that the space–time theory of gravitation plays any direct role in establishing physically correct transformations.

The principle of general space–time covariance appears as a necessary mathematical facility which is able to accommodate within the realm of its formalism the realistic as well as the unrealistic transformations. Galilean or Lorentz translations, Galilean-type (absolute time) rotations or rotations of the form (11) or (24), are all equally permissible from a mathematical point of view, because all of them are subgroups contained in the set of general space–time transformations implied by the principle of general covariance.

IV. GEOMETRIC OPTICAL THEORY

The previous section treated with higher-order detail the geometric optical theory of the Sagnac effect for a very simplified physical arrangement. We learned that higher-order effects can be neglected for all practical experimental purposes. We may now attack the problem of a general first-order geometric optical analysis of more realistic experimental configurations of interferometers and ring lasers, including cases having optically refracting materials in the path of the light beams.

It is convenient to define first the meaning of the symbols that occur in the following derivations:

- ϕ = phase of the wave front of the light beam in radians.
- Z = path measured in wavelengths also called the mode number in the case of a self-oscillating system.
- δZ = fringe shift associated with a comparison of the moving and the stationary system.
- ΔZ = fringe shift associated with interference of clockwise and counterclockwise beams.
- n = index of refraction of the stationary medium.
- $\mathbf{k}$ = wave vector in medium.
- k = wave number in medium $k^2 = \mathbf{k}\cdot\mathbf{k}$.
- $k_0 = k/n$, free-space wave number.
- $\lambda = 2\pi/k$, wavelength in medium.
- $\lambda_0 = \lambda n$, free-space wavelength.
- ω = circular frequency.
- $\nu = \omega/2\pi$ frequency.
- $d\mathbf{r}$ = vector line element.
- ds = scalar line element $ds^2 = d\mathbf{r}\cdot d\mathbf{r}$.
- τ = circulation time for the light for stationary loop.
- $\delta\tau$ = change of circulation time with respect to the stationary case.

$\Delta\tau$ = difference in circulation time between clockwise and counterclockwise circulation.
$\mathbf{v}$ = velocity field
$\mathbf{q}$ = displacement vector generated by $\mathbf{v}$.
$u = c/n$, phase velocity in medium.
c = free-space velocity.

The phase expression for the light beam after one circulation in a closed loop of arbitrary shape is

$$\phi = \frac{1}{2\pi}\oint \mathbf{k}\cdot d\mathbf{r} - \frac{1}{2\pi}\int_0 \omega\, dt. \tag{31}$$

The first integral in Eq. (31) counts the number of wavelengths in the closed spatial path, the second integral gives the number or radians over which the monochromatic signal advances during the time needed for one circulation. The spatial part of the line integral is closed, whereas the time part is not closed.

Expression (31) is a space–time line integral which could have been easily rendered in the general-invariant form $\int k_\lambda\, dx^\lambda$, if k_λ, for $\lambda = 0, 1, 2, 3$, is considered as the four-vector of frequency and wave number. For the present purpose it is more practical to retain the conventional spatial form. Multiplication by Planck's constant h converts (31) into a Hamilton action integral

$$\oint \mathbf{p}\cdot d\mathbf{r} - \int H\, dt = \int L\, dt, \qquad (L = \text{Lagrangian}) \tag{32}$$

with $(-H, \mathbf{p})$ the four-vector of energy-momentum, showing the action and phase to be related invariants for general space–time transformations.

Now we suppose that the constraint (that is the interferometer), forcing the light to circulate in a closed loop, is subjected to a small time-dependent displacement $\mathbf{q}$, generated by the velocity $\mathbf{v}$. The phase ϕ is a general invariant and should not be affected by this displacement provided we properly account for the variation of the boundaries. We thus find

$$\delta\phi = \delta Z - \delta T = 0, \tag{33}$$

where

$$2\pi\delta Z = \delta\oint \mathbf{k}\cdot d\mathbf{r}$$

$$= \oint \{\delta\mathbf{k} - \mathbf{q}\times \operatorname{curl}\mathbf{k} + \operatorname{grad}(\mathbf{k}\cdot\mathbf{q})\}\cdot d\mathbf{r} \tag{34}$$

and

$$2\pi\delta T = \delta\int_0 \omega\, dt = \int_0 \delta\omega\, dt + \omega\delta\tau. \tag{35}$$

The variation of the spatial part of the space–time line integral (31) as given by Eq. (34) is based on a well-known formula (Madelung, 1943, and Brandstatter, 1963) which gives the variation of a line integral as the result of a deformation field $\mathbf{q}$. The variation is expressed in terms of parameters that relate to a frame of reference in which the stationary system is described (inertial frame). We assume for the interferometer that we are dealing with a situation for which geometric optical conditions prevail. We may then apply the Sommerfeld–Runge law which says that (Poeverlein, 1962)

$$\operatorname{curl}\mathbf{k} = 0. \tag{36}$$

Using (36) and integrating the last term in (34) one obtains for δZ

$$2\pi\delta Z = \oint \delta\mathbf{k}\cdot d\mathbf{r} + (\mathbf{k}\cdot\mathbf{q})_2 - (\mathbf{k}\cdot\mathbf{q})_1. \tag{37}$$

The suffixes (2) and (1) in Eq. (37) denote the values of the scalar product $(\mathbf{k}\cdot\mathbf{q})$ at the end and at the beginning of one circulation around the loop. It is important to note that $\mathbf{q}$ is not single valued for a circulation around the loop because the deformation increases with time.

Equation (37) represents the change in path length Z in terms of the wavelength as compared with the value of Z for the stationary loop. This change δZ is simply the fringe shift associated with the velocity field $\mathbf{v}$. The first part gives the "intrinsic" change of the wave vector due to $\mathbf{v}$ and the last part is the contribution due to the change of the boundaries of the integral.

We could have taken the variation of Z as the starting point of a conventional spatial discussion of the fringe-shift problem. It will appear that the space–time generalization comes in handy for future use.

A general space–time variation of ϕ yields, along with the Sommerfeld–Runge law, the Hamilton equations of motion for the light rays. The Hamilton equations plus the Sommerfeld–Runge law are mathematically the necessary and sufficient conditions that make the four-vector of frequency and wave number curl free in a space–time sense. This property makes the integrand of the space–time line integral (31) for the phase ϕ a total differential for the permissible trajectories. We do not explicitly need these Hamilton equations for the present purpose. It is sufficient to assume for the actual trajectories of the light beams in the interometer that they follow simple straight lines between the mirrors. The Hamilton equations for the light ray become operational only if the frequency is a function of position and if the medium is dispersive. Unless specifically stated, neither is the case in the following applications. The Sommerfeld–Runge law then remains as the operationally more important dynamical condition for light rays.

We now evaluate the fringe shift for the ring interferometer and the frequency shift for the ring laser

from relations (35) and (37) by applying the appropriate accessory conditions corresponding to the experimental situations.

A. The Moving Ring Interferometer with Comoving Medium

The accessory condition for the ring interferometer is

$$\delta\omega = 0, \tag{38}$$

because the external light source determines unambiguously the light frequency occurring in the interferometer. For the light source moving with the interferometer it is obvious that (38) should hold. If the light source is stationary it is possible, depending on the experimental arrangement, that a Doppler shift occurs due to the motion. This Doppler shift affects clockwise and counterclockwise beams both in the same manner so that the fringe shift is only affected in higher orders; equal frequencies, that is, $\delta\omega = 0$, are still necessary for interference.

The relation between ω, k and the phase velocity u in a linear medium is given by

$$\omega = ku. \tag{39}$$

Taking into account (38) this yields

$$\delta k/k = -\delta u/u, \tag{40}$$

in which δu is the change in effective propagation velocity in the moving medium as seen by the stationary observer. In first approximation one may assume that δu is given by an expression of the form

$$\delta u = \alpha \mathbf{v}\cdot d\mathbf{r}/ds, \tag{41}$$

in which α is a coefficient of drag, similar to but not necessarily identical with the Fresnel-Fizeau coefficient of drag for translational motion; $d\mathbf{r}/ds$ is the unit vector tangent to the direction of the beam.

It follows from (40) and (41) that

$$\delta k = -(k/u)\alpha \mathbf{v}\cdot(d\mathbf{r}/ds). \tag{42}$$

The integrand in (37) gives $\delta\mathbf{k}$ in the direction of $d\mathbf{r}$ and (42) gives the change of $\mathbf{k}$ in that same direction; hence substitution in (37) yields

$$\delta Z = -\frac{1}{2\pi}\oint \alpha \frac{k}{u}\mathbf{v}\cdot d\mathbf{r} + \frac{1}{2\pi}\{(\mathbf{k}\cdot\mathbf{q})_2 - (\mathbf{k}\cdot\mathbf{q})_1\}. \tag{43}$$

The last two terms in (43) can be expressed in the velocity field $\mathbf{v}$ if one considers that $(\mathbf{k}\cdot\mathbf{q})$ changes over the interval of time dt by the amount $\mathbf{k}\cdot\mathbf{v}\,dt$. Hence going around the complete loop one obtains

$$(\mathbf{k}\cdot\mathbf{q})_2 - (\mathbf{k}\cdot\mathbf{q})_1 = \int_0 \mathbf{k}\cdot\mathbf{v}\,dt = \oint \mathbf{k}\cdot\mathbf{v}\frac{ds}{u} = \oint \frac{k}{u}\mathbf{v}\cdot d\mathbf{r}, \tag{44}$$

in which one uses the fact that k and $d\mathbf{r}$ have the same direction.

A substitution of (44) in (43) gives

$$\delta Z = \frac{1}{2\pi}\oint \frac{k}{u}(1-\alpha)\mathbf{v}\cdot d\mathbf{r}. \tag{45}$$

Expression (45) is not yet the observed result because δZ is the fringe shift that would occur if the circulating beam in the stationary interferometer could interfere with one of the circulating beams in the moving interferometer. When the interferometer is in motion there will also be a beam going in the opposite direction around the loop. Inspection of (45) shows that the beam going in the opposite direction around the loop has a fringe shift δZ of the opposite sign. In the moving interferometer only the two distinct clockwise and counterclockwise beams occur simultaneously—the observed fringes between these beams are shifted by twice the amount δZ in comparison with the fringe position for the stationary interferometer. This simple procedure of doubling the result (45) is valid only if the loop in the stationary case has reciprocal properties, which means there is complete mode degeneracy for the clockwise and counterclockwise beams, because the propagation properties in the opposite direction are the same, when the interferometer is stationary.

Introducing the free-space parameters c and λ_0, one thus finds for the actually observed fringe shift ΔZ, produced by the clockwise and counterclockwise beams in the moving interferometer with comoving medium, when compared with the fringe position for the stationary interferometer

$$\Delta Z = \frac{2}{c\lambda_0}\oint n^2(1-\alpha)\mathbf{v}\cdot d\mathbf{r}. \tag{46}$$

From Eq. (46) one can derive very simply the difference in circulation time between the clockwise and counterclockwise beams. It follows from (33) and (35) and the accessory condition (38) that

$$\omega\delta\tau = 2\pi\delta Z, \tag{47}$$

where $\delta\tau$ is again the change in loop circulation time for the clockwise beam, compared with the stationary case. We now define, in a similar manner to the case of the fringe shift, $\Delta\tau$ as the difference in circulation time between the clockwise and counterclockwise beams, thus leading to the corresponding relation

$$\omega\Delta\tau = 2\pi\Delta Z. \tag{47a}$$

From (46) we then obtain for

$$\Delta\tau = \frac{2}{c^2}\oint n^2(1-\alpha)\mathbf{v}\cdot d\mathbf{r} \tag{48}$$

in the moving interferometer with comoving optical medium.

B. The Moving Ring Laser with Comoving Medium

For the ring laser we need instead of (38) an accessory condition which states that the phase going around the loop should be univalued for sustained oscillation. If one excludes the possibility of mode jumping as a result of the motion of the ring laser (an experimentally easily detectable occurrence) one thus imposes the condition that the number of wavelengths in the loop should remain constant (constant mode number)

$$\delta Z = 0. \tag{49}$$

It then follows from (33) that $\delta T = 0$ or from Eq. (35)

$$\int_0 \delta\omega \, dt + \omega \, \delta\tau = 0. \tag{50}$$

For a uniform and stationary motion $\delta\omega$, which is now different from zero, should be constant. It then follows from (50) that

$$\delta\omega/\omega = -\delta\tau/\tau; \tag{50a}$$

and following the now familiar doubling procedure for the frequency and transition time difference between the clockwise and counterclockwise modes

$$|\Delta\omega/\omega| = \Delta\tau/\tau. \tag{50b}$$

The difference in the circulation times between the clockwise and counterclockwise beams does not depend on whether the optical circuit is being used as an interferometer or as a ring laser. Hence using Eq. (48) one obtains

$$\left|\frac{\Delta\omega}{\omega}\right| = \left(2\oint n^2(1-\alpha)\mathbf{v}\cdot d\mathbf{r}\right) \Big/ c\oint n\, ds \tag{51}$$

in which τ has been expressed in the path length and propagation velocity through the Fermat integral

$$\tau = \oint \frac{ds}{c/n}. \tag{52}$$

The logically more consistent, but also more lengthy procedure for deriving (51) is to start from $\delta Z = 0$ and eliminate δk by means of the relation $\delta k/k = \delta\omega/\omega - \delta u/u$, which leads to the same result (51).

C. The Moving Interferometer and Ring Laser with a Stationary Medium in the Beam Path

The starting point for the discussion is again formula (37) except that according to (40) the change in the wave vector δk should vanish, because δu vanishes when observing the propagation velocity in the medium from a frame of reference in which the medium rests. The fringe shift ΔZ is then given by

$$\Delta Z = \frac{2}{c\lambda_0}\oint n^2\mathbf{v}\cdot d\mathbf{r}, \tag{53}$$

which is (46) for zero drag, that is, $\alpha = 0$.

Evaluation of the integral in (53) is cumbersome if the stationary medium does not completely fill the path of the light beams between the mirrors of the interferometer.

Similar arguments apply to the self-oscillating case. The corresponding formula for the beat frequency is

$$\frac{\Delta\omega}{\omega} = \frac{2}{c}\left(\oint n^2\mathbf{v}\cdot d\mathbf{r} \Big/ \oint n\, ds\right). \tag{54}$$

Prunier and Dufour (1942) performed an experiment with a rotating ring interferometer in which the light was flashed through stationary glass rods. For practical reasons they had to permit an airgap in the beam path.

D. The Stationary Ring Interferometer and Ring Laser with a Moving Medium in the Beam Path

Going back to formula (37) we now have a situation, which is due to the motion of the loop, in which the integrated parts vanish because the loop is stationary. The fringe shift is now due solely to the phenomenon of drag given by the integral in (37). The fringe shift then becomes, through the use of (42),

$$\Delta Z = \frac{2}{c\lambda_0}\oint n^2\alpha\mathbf{v}\cdot d\mathbf{r} \tag{55}$$

and the corresponding beat frequency for the ring laser

$$\frac{\Delta\omega}{\omega} = \frac{2}{c}\left(\oint n^2\alpha\mathbf{v}\cdot d\mathbf{r} \Big/ \oint n\, ds\right). \tag{56}$$

Expression (55) represents the well known Fresnel-Fizeau effect for a translational motion. A rotational version of this experiment has apparently not yet been made. Such an experiment would not be altogether trivial because it could inform us about the extent to which the translational coefficient of drag can be extrapolated to cases of nonuniform motion.

E. Two Formulas for Ring Lasers

Finally we give two explicit cases: the triangular and the square ring laser of main dimensions D and a comoving slug of optical material of length d in the beam path. The coefficient of drag α is given by (2). without the dispersion term, that is, $\alpha = 1 - n^{-2}$.

An application of formula (51) for the triangular ring laser gives (see Fig. 9)

$$\frac{\Delta\omega}{\omega} = \frac{\sqrt{3}\Omega D}{c\{3 + (n-1)(d/D)\}} \tag{57}$$

for the ring laser formed by an equilateral triangle.

The corresponding formula for the square ring laser is (see Fig. 10)

$$\frac{\Delta\omega}{\omega}=\frac{4\Omega D}{c\{4+(n-1)(d/D)\}}. \tag{58}$$

The length of the slug d and the index of refraction occur as a product in the denominator so that an increase of either d or n has the same effect. The relative frequency shift $\Delta\omega/\omega$ is, according to the theory, independent of the position of the slug in the beam path.

To evaluate expression (51) it is advantageous to apply Stokes theorem to the line integral

$$\oint \mathbf{v}\cdot d\mathbf{r}=\oint \text{curl}\,\mathbf{v}\cdot d\mathbf{A}=2\boldsymbol{\Omega}\cdot\mathbf{A}. \tag{59}$$

One uses here the well-known property of a purely rotational field $\mathbf{v}$

$$\text{curl}\,\mathbf{v}=2\boldsymbol{\Omega}, \tag{60}$$

whereby $\boldsymbol{\Omega}$ is the vector that gives the direction and the rate of rotation. The constancy of $\boldsymbol{\Omega}$ in relation (60) accounts for the independence of the Sagnac effect from the center around which the equipment is being rotated.

The original Sagnac formula (1) is obtained from (46) by taking $\alpha=1-n^{-2}$ and by using the relations (59) and (60).

The beat frequency of a ring laser, unlike the fringe shift of the ring interferometer, depends on the properties of the comoving medium traversed by the beams. Khromykh (1966) has pointed out that therefore the dispersion can also affect the observed beat frequency. Later considerations show (mentioned under the heading Consistency Checks) that the dispersion comes into the final result only through the denominator of (51). The index of refraction for the clockwise mode differs from the index of refraction of the counterclockwise mode because of the frequency difference between the two modes. On making a Taylor expansion of the index of refraction n around the center frequency, one finds that the first-order term $(dn/d\omega)$ drops out, while the second derivative $d^2n/d\omega^2$ remains. The contribution of this second-order term near a point of anomalous dispersion, as does occur in a "lasing" medium, may not be quite negligible.

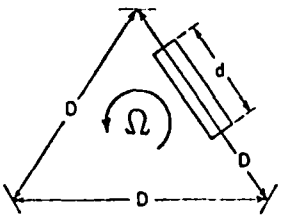

FIG. 9. Triangular ring laser with comoving medium in the beam path.

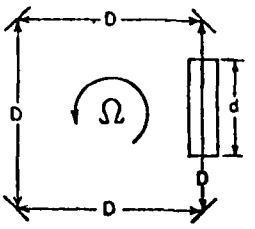

FIG. 10. Square ring laser with comoving medium in the beam path.

F. Consistency Checks

To be consistent with the principle of relativity one has to demand that the Sagnac interferometer and the ring laser cannot lead to a fringe shift or a beat frequency if the equipment is in uniform translational motion. An inspection of formulas (46) and (51) shows that it is necessary and sufficient to require that

$$\oint n^2(1-\alpha)\mathbf{v}\cdot d\mathbf{r}=0, \tag{61}$$

if $\mathbf{v}$ is a uniform translational velocity field.

It is known that

$$\oint \mathbf{v}\cdot d\mathbf{r}=0, \tag{62}$$

if $\mathbf{v}$ is a uniform translational velocity.

Relations (61) and (62) are compatible if and only if

$$n^2(1-\alpha)=C=(\text{constant}). \tag{63}$$

Hence the coefficient of drag is

$$\alpha=1-C/n^2, \tag{64}$$

which is of the form required by the Fresnel-Fizeau effect. The constant C is known to equal one for a purely translational motion of uniform velocity.

For another consistency check we may consider formulas (53) and (55). Equation (53) gives the fringe shift for a stationary material medium and a moving interferometer, while Eq. (55) gives the fringe shift for a moving medium and a stationary interferometer. The fringe shifts given by these two formulas should be the same if the velocity field $\mathbf{v}$ is a uniform translation, because then both formulas describe the conventional Fresnel-Fizeau effect.

Equation (53) is given by

$$\Delta Z=\frac{2}{c\lambda_0}\oint n^2\mathbf{v}\cdot d\mathbf{r} \tag{65}$$

and Eq. (55) becomes after substituting Eq. (64)

$$\Delta Z=\frac{2}{c\lambda_0}\oint n^2\mathbf{v}\cdot d\mathbf{r}-\frac{2C}{c\lambda_0}\oint \mathbf{v}\cdot d\mathbf{r}. \tag{66}$$

For arbitrary contours of the integrals and for an arbitrary dependence of n on position, one finds that expressions (65) and (66) can be equal and nonzero, if and only if $\mathbf{v}$ is a uniform translational velocity field, because then the last integral in (66) vanishes.

Equations (65) and (66) demonstrate the breakdown of the principle of relativity for nonuniform motion.

A simple, but amusing demonstration is that Eq. (51) is also compatible with the red shift if $\mathbf{v}$ is a uniformly accelerated motion. The index of refraction drops out of the end result as it should.

V. PHYSICAL OPTICAL THEORY

A. Constitutive Relations and Maxwell Equations

A physical optical theory of the Sagnac effect requires an application of electromagnetic theory to rotating or in general to nonuniformly moving systems. The traditional text book form of Maxwell theory is, for a number of reasons, poorly suited for such an endeavor. The most important of these reasons is:

(1) The traditional space-time formulations of the Maxwell equations do not make sufficiently explicit the constitutive properties of free space.

(2) It is not possible as in the case of uniformly translating systems to consider solely the mutual motion of observer and object. A recasting of Maxwell theory so that we can clearly delineate the physical and mathematical steps associated with these two points is necessary.

While it is common practice to speak of constitutive equations for a material electromagnetic medium, it is not customary to speak of constitutive relations for free space, because it is traditionally assumed that there is no physical distinction between dielectric displacement $\mathbf{D}$ and electric field $\mathbf{E}$ nor between magnetic induction $\mathbf{B}$ and magnetic field $\mathbf{H}$ in free space. The basic argument for justifying this so-called Gaussian field identification stems from the apparent absence of any material polarization mechanisms in free space. Dimensional considerations support the idea of at least a formal distinction between the field vectors in free space. The same is true for arguments based on mathematical invariance. Neither the dimensional nor the invariance features have been accepted as physically sufficiently compelling to abandon the electromagnetic field identification in free space.

The absence of a field distinction between $\mathbf{E}$, $\mathbf{D}$ and $\mathbf{H}$, $\mathbf{B}$ in vacuum in customary discussions of Maxwell's theory must be considered as a flaw, because it sweeps the medium aspects of free space under the rug. In fact, the identification $\mathbf{E}=\mathbf{D}$ and $\mathbf{B}=\mathbf{H}$ may be said to define the electromagnetic properties of free space, only as seen from inertial frames because the field identification, in conjunction with the Maxwell equations, leads to the standard free-space d'Alembertian wave equation which is a Lorentz invariant structure.

A d'Alembertian wave equation can, in no way whatever, explain the nonreciprocal asymmetry between the clockwise and counterclockwise beams observed in the Sagnac effect, because a nonreciprocity requires the presence of mixed space–time derivatives $(\partial/\partial t\ \partial x)$ in the wave equation. Thus in order to account for the asymmetry one has to assume that either the Gaussian field identification does not hold in a rotating frame or that the Maxwell equations are affected by rotation.

All existing evidence for the treatment of nonreciprocal phenomena in material media points in the direction of modified constitutive relations, not modified Maxwell equations. In fact, the Maxwell equations, as the universal laws of macroelectromagnetics, are expected to apply to any medium regardless of the symmetry properties of that medium and regardless of the mutual motion of the frame of reference and the medium. A detectable mutual motion of medium and frame of reference reveals a lack of space–time symmetry. Free space has the interesting space–time symmetry property which says that uniform translations cannot be detected. This space–time symmetry is characterized by the Lorentz group.

It is particularly true that the Gaussian field identification is a Lorentz invariant identification. Conversely, the invariance of the field identification can be used to define the Lorentz group. This becomes clear if one realizes that the Minkowskian six-vectors $\mathbf{E}$, $\mathbf{B}$ and $\mathbf{D}$, $\mathbf{H}$ in free space are related by the space–time metric. Insisting on the Gaussian field identification is then equivalent to an insistance on the invariance of the Minkowskian metric $(c^2, -1, -1, -1)$. This invariance defines the Lorentz group as a symmetry property of the space–time continuum for uniform translations.

The common assertion that the Maxwell equations have a built-in Lorentz invariance holds by virtue of the Gaussian field identification $\mathbf{E}=\mathbf{D}$, $\mathbf{H}=\mathbf{B}$ (or $\mathbf{D}=\epsilon_0\mathbf{E}$ and $\mathbf{B}=\mu_0\mathbf{H}$, with ϵ_0 and μ_0 constants). It was therefore Gauss who, perhaps unwittingly, injected this (special) relativistic element into the Maxwellian theory for free space, simply by the tacit suggestion that the free-space identification would be valid in any frame of reference regardless of its state of motion. We see from the present considerations that the latter extrapolation (identification for any state of motion including accelerated motion) is mathematically impossible if one demands for logical and methodological reasons that the free-space properties should also be given by a set of free-space constitutive relations while the Maxwell equations are not affected.

The methodological objective of functionally separating constitutive relations and Maxwell equations is

only possible if the Maxwell equations, when written with four field vectors **E**, **D**, **B**, and **H**, indeed obey a much wider invariance group than the Lorentz group. In fact, the invariance group of the Maxwell equations with four spatial vectors should be a covering group of all conceivable space–time symmetries that can physically exist.

Weyl and Cartan recognized quite early the metric independent form invariance of the Maxwell equations for the set of general, nonlinear, space–time transformations. The metric independence of this invariance is important because the space–time metric represents the electromagnetic structural properties of free space. If the metric still appeared in the Maxwell equations, for instance in the form of a covariant derivative, it would mean that the free-space constitutive properties have not been properly extracted from the Maxwell equations. We owe to Cartan (1924) and Weyl (1951) the observation that this separation of fundamental laws and constitutive properties is indeed possible for the theory of electromagnetism. [A careful reading of pages 110 and 220 of Weyl (1951) shows Weyl's awareness of the metric independent form. Cartain (1924, p. 19) states very specifically: "Les equations de Maxwell sont independantes de toute hypothese sur la connection affine de l'espace-temps." The first publication of Weyl's book was in 1918.]

The Maxwell equations are not commonly presented in the Cartan-Weyl form. In comparison with the customary Minkowskian form, all that is needed to bring about the Cartan–Weyl form is, that **E**, **B** constitute a covariant six-vector $F_{\lambda\nu}$, while **D**, **H** constitute a contraviant six-vector density $\mathcal{G}^{\lambda\nu}$ of weight $+1$. The metric independent form of the equations is then

$$\partial_{[\kappa}F_{\lambda\nu]}=0 \tag{67}$$

$$\partial_\nu \mathcal{G}^{\lambda\nu}=\mathcal{C}^\lambda. \tag{68}$$

The only difference with respect to more customary versions is that $\mathcal{G}^{\lambda\nu}$ is regarded as a density of weight $+1$, which is really in keeping with the true physical nature of the quantities involved, because the four-vector of the charge and current density $\mathcal{C}^\lambda$ is at least spatially a true density. The customary versions $\mathcal{G}^{\lambda\nu}=g^{1/2}G^{\lambda\nu}$ and $\mathcal{C}^\lambda=g^{1/2}c^\lambda$ (g=determinant of the metric) do not make this physical feature of the fields explicit. The derivatives in the Eqs. (67) and (68) are ordinary partial derivatives not covariant derivatives.

Van Dantzig (1934), who later rediscovered this interesting property of the Maxwell equations, further developed this into a method, which might be called the method based on the principle of metric independence. An interesting dimensional substantiation of van Dantzig's method was later given by Dorgelo and Schouten (1946).

Van Dantzig (1934) also introduced constitutive relations between $\mathcal{G}^{\lambda\nu}$ and $F_{\lambda\nu}$ and noted that in general they have the form of integral relations in order to express the noninstantaneous and nonlocal relations between applied fields and polarizations.

The most general linear algebraic relations that can occur between $\mathcal{G}^{\lambda\nu}$ and $F_{\lambda\nu}$ are

$$\mathcal{G}^{\lambda\nu}=\tfrac{1}{2}\chi^{\lambda\nu\sigma\kappa}F_{\sigma\kappa} \tag{69}$$

where $\chi^{\lambda\nu\sigma\kappa}$ is called the constitutive tensor. [This tensor obeys the symmetry properties $\chi^{\lambda\nu\sigma\kappa}=-\chi^{\nu\lambda\sigma\kappa}=\chi^{\sigma\kappa\lambda\nu}$. [Chapter VI of Post (1962) gives a detailed discussion.]

The first Maxwell equation as usual implies that $F_{\lambda\nu}$ can be derived from a potential vector A_ν according to

$$F_{\lambda\nu}=2\partial_{[\lambda}A_{\nu]}. \tag{70}$$

Substitution of (70) in (69) and (69) in (68) yields the *generally invariant vector d'Alembertian* (*wave equation*)

$$\partial_\nu\chi^{\lambda\nu\sigma\kappa}\partial_\sigma A_\kappa=0, \tag{71}$$

where we have assumed $\mathcal{C}^\lambda=0$.

The derivatives in Eq. (71) are ordinary partial derivatives, not covariant derivatives. Equation (71) is nevertheless valid for any curvilinear system of coordinates, provided we transform χ as implied by the invariance of Eq. (69), that is, χ is a tensor density.

We may now use Eq. (71) for a physical optical analysis of the Sagnac effect in free space and in a medium, whereby we also consider the case where the medium rotates with the mirror system as well as the case where the medium is stationary while the mirrors rotate and finally the case where the mirrors are stationary but the medium rotates.

As in the geometric optic treatment, there are two ways of attacking the problem. One writes the Eqs. (71) for an inertial frame of reference whereby the boundary conditions become time dependent due to the motion of the mirrors and the beam splitter (wave launcher), or one computes Eq. (71) for a rotating frame where the boundary conditions in the rotating frame retain their familiar time-independent form. We follow the latter approach here.

This program makes it necessary to evaluate the coefficients of the constitutive tensor for moving frames of reference and for moving media, which brings up the most crucial and incisive distinctions between the theory of uniformly translating and nonuniformly moving systems.

For the theory of the uniformly translating systems it is immaterial whether one considers the medium to be moving with respect to the frame of reference of the observer or whether one considers the frame of refer-

ence to be moving with respect to the medium, because a translatory motion does not generate any intrinsic physical changes in the body as long as the translation is uniform.

For nonuniformly moving systems it is mandatory to distinguish between the motion of the object (medium), and the motion of the observer (frame of reference). The principle of relativity breaks down for nonuniform motion. A nonuniform motion produces a real and intrinsic physical change in the object in motion; the motion of the frame of reference by contrast produces solely a difference in the observational viewpoint.

We may substantiate the above statements shortly by giving three rather well-known examples that clearly demonstrate the physical necessity of distinguishing between the nonuniform motions of the object and the observer.

We will see that the uniform or nonuniform motions of the observer are covered by the principle of general covariance and the tensorial behavior of the fields for general space–time transformations. This purely observational change in point of view does not generate any intrinsic physical changes in the object.

A nonuniform motion of an object that is under observation from a frame of reference, inertial or noninertial, produces real intrinsic physical changes in that object. For instance a rotating disk becomes electrically polarized in the radial direction. A rotating magnetizable bar becomes magnetized in its axial direction (Barnett experiment), although neither the disk nor the bar shows any field whatsoever when at rest in an inertial frame. These fields are produced by rotation where initially, when at rest, there was no field at all. This is a typically nontensorial feature which could not possibly be covered by an indiscriminate application of the principle of general covariance in conjunction with the known tensorial characteristics of the electromagnetic field.

The three examples which clearly illustrate this necessary distinction for nonuniform motion are:

(1) The Barnett (1915) experiment, rotating the magnetizable bar or rotating the frame of reference instead of the bar are clearly different operations from a physical point of view. Rotation of the bar gives magnetization; rotation of the frame of reference does not.

(2) The Oppenheimer paradox (Schiff, 1939): rotating a charged spherical condenser or rotating the frame of reference instead of the condenser are physically different operations. Rotation of the condenser produces an external magnetic field; rotation of the frame of reference does not.

(3) The rotational Fresnel-Fizeau experiment (medium rotating, mirrors stationary) and the Dufour-Prunier (1942) experiment (medium stationary mirrors rotating) are physically not equivalent [compare the discussion of Eqs. (65) and (66) of Sec. IV of this paper].

B. Constitutive Relations for Rotating Systems

In the previous discussion a major point was made of the fact that the intrinsic properties of a medium can be affected by a rotation. This implies that the constitutive properties when measured while observer and medium both are at rest in the same rotating frame are not exactly the same as those observed when observer and medium both are at rest in the same inertial frame. In a rotating body, a radial polarization is deflected by Coriolis forces, thus causing a change in the axial magnetization, and vice versa. It is known, however, that the magnetization of optical materials is negligible for all practical purposes. Thence, if we neglect the not easily calculable intrinsic influence of the rotation on the medium, we may expect the results of the physical optical analysis to be consistent with the results of the geometric optical analysis, for all media with $\mu_r=1$.

To obtain Eqs. (71) for the rotating frame, it is necessary to express the constitutive tensor χ with respect to the rotating frame. To do this one must have a frame of reference for which χ is known. The free-space case is simple enough, χ on a Cartesian inertial frame is given by

$\chi^{\lambda\nu\kappa\epsilon}$	E	B
−D	$-\epsilon_0$	0
H	0	$1/\mu_0$

. (72)

Similarly for an isotropic medium with relative permittivity ϵ_r, relative permeability μ_r, and at rest in an inertial frame, we have

$\chi^{\lambda\nu\kappa\epsilon}$	E	B
−D	$-\epsilon_0\epsilon_r$	0
H	0	$1/(\mu_0\mu_r)$

. (73)

For the following applications it is necessary to separate the constitutive tensor χ into its "free-space" part and the part due to the polarizability of the medium, "the material part," because depending on the physical situation each part may be known in different frames.

The free-space part of χ which is known to have the form (72) in an inertial frame, when seen from a rotating frame, must now be transformed. For a Galilei rotation of rate Ω around the Z axis, *while*

simultaneously making a transition to cylindrical coordinates, one has:

Free Space Observed from Rotating Frame

$\chi^{\lambda\nu\sigma\kappa}$	E_r	E_ϕ	E_z	B_r	B_ϕ	B_z
$-D_r$	$-\epsilon_0 r$	0	0	0	0	$r\Omega\epsilon_0$
$-D_\phi$	0	$-\epsilon_0/r$	0	0	0	0
$-D_z$	0	0	$-\epsilon_0 r$	$-r\Omega\epsilon_0$	0	0
H_r	0	0	$-r\Omega\epsilon_0$	$1/(\mu_0 r)$	0	0
H_ϕ	0	0	0	0	r/μ_0	0
H_z	$r\Omega\epsilon_0$	0	0	0		$1/(\mu_0 r)$

(74)

The case of the stationary material medium, which in the stationary frame is given by (73), is converted into (75) when seen from a rotating frame of cylindrical coordinates. To obtain (75) it is only necessary to replace ϵ_ϕ by $\epsilon_r\epsilon_0$ and μ_0 by $\mu_0\mu_r$ in (74).

Stationary Medium Observed from Rotating Frame

$\chi^{\lambda\nu\sigma\kappa}$	E_r	E_ϕ	E_z	B_r	B_ϕ	B_z
$-D_r$	$-r\epsilon_0\epsilon_r$	0	0	0	0	$r\Omega\epsilon_0\epsilon_r$
$-D_\phi$	0	$-\epsilon_0\epsilon_r/r$	0	0	0	0
$-D_z$	0	0	$-r\epsilon_0\epsilon_r$	$-r\Omega\epsilon_0\epsilon_r$	0	0
H_r	0	0	$-r\Omega\epsilon_0\epsilon_r$	$1/(\mu_0\mu_r r)$	0	0
H_ϕ	0	0	0	0	$r/(\mu_0\mu_r)$	0
H_z	$r\Omega\epsilon_0\epsilon_r$	0	0	0	0	$1/(\mu_0\mu_r r)$

(75)

Where we have transformed free-space and medium part together it should be clear that (75) describes the case where the medium is stationary in the inertial frame and the whole thing (inertial free space and material medium) is observed from the rotating frame. This corresponds to the Dufour–Prunier experiment discussed earlier in Secs. II and IV.

Now let us suppose that the medium rotates with the mirrors. It would then be wrong to transform the material part of χ because the medium is stationary in the frame of reference, although there may occur intrinsic changes of the material part which may be neglected for $\mu_r = 1$. The free-space part of the constitutive tensor, which in the inertial frame is given by (72), when viewed from the rotating frame is still given by (74). It then follows for the corotating material medium, if we neglect the intrinsic changes of the material part:

Corotating Medium, Intrinsic Changes of Material Part Neglected

$\chi^{\lambda\nu\sigma\kappa}$	E_r	E_ϕ	E_z	B_r	B_ϕ	B_z
$-D_r$	$-r\epsilon_0\epsilon_r$	0	0	0	0	$+r\Omega\epsilon_0$
$-D_\phi$	0	$-\epsilon_0\epsilon_r/r$	0	0	0	0
$-D_z$	0	0	$-r\epsilon_0\epsilon_r$	$-r\Omega\epsilon_0$	0	0
H_r	0	0	$-r\Omega\epsilon_0$	$1/(\mu_0\mu_r r)$	0	0
H_ϕ	0	0	0	0	$r/(\mu_0\mu_r)$	0
H_z	$+r\Omega\epsilon_0$	0	0	0	0	$1/(\mu_0\mu_r r)$

(76)

In the same way we can obtain the constitutive tensor for the rotating medium while it is being observed by a stationary interferometer (Fresnel–Fizeau effect). The observation being made in an inertial frame implies that the free-space part retains the form (72); the medium part on the rotating frame has the form $\epsilon_0(\epsilon_r-1)$ and $\mu_0(\mu_r-1)$ if we again discard the intrinsic changes. When the rotating medium is viewed from the inertial frame, however, one obtains off-diagonal terms, because the inertial frame observer rotates in the opposite direction with respect to the medium that is in absolute motion. Adding the unaffected free-space part one finds:

Rotating Medium Viewed from Inertial Frame, Intrinsic Changes Neglected

$\chi^{\lambda\nu\sigma\kappa}$	E_r	E_ϕ	E_z	B_r	B_ϕ	B_z
$-D_r$	$-r\epsilon_0\epsilon_r$	0	0	0	0	$-r\Omega\epsilon_0(\epsilon_r-1)$
$-D_\phi$	0	$-\epsilon_0\epsilon_r/r$	0	0	0	0
$-D_z$	0	0	$-r\epsilon_0\epsilon_r$	$r\Omega\epsilon_0(\epsilon_r-1)$	0	0
H_r	0	0	$r\Omega\epsilon_0(\epsilon_r-1)$	$1/(r\mu_0\mu_r)$	0	0
H_ϕ	0	0	0	0	$r/\mu_0\mu_r$	0
H_z	$-r\Omega\epsilon_0(\epsilon_r-1)$	0	0	0	0	$1/(r\mu_0\mu_r)$

(77)

A few remarks may be appropriate with regard to the physical meaning of the constitutive relations implied by (74), (75), (76), and (77). In the next section we will see that (74) leads to the familiar Sagnac result in vacuum, while (75), (76), and (77) will lead to results identical to those obtained earlier, provided $\mu_r=1$. For the free-space case it seems a legitimate question whether a cross-effect as suggested by (74) really exists. It is important to note that (72) is invariant under a Lorentz transformation; the cross relation between electric and magnetic field suggested by the off-diagonal terms in (74) would thus be typical for a rotational motion.

Pegram (1917) performed an experiment that seems to give some relevant information of how these off-diagonal terms can be observed. He rotates, simultaneously and around the same axis, a coaxial cylindrical condenser and solenoid. The solenoid is energized and gives a magnetic field in the axial direction between the plates of the condenser. A temporary shorting of the plates while rotating, will give a charge to the condenser [according to the upper right hand term in (74)]. This charge can be observed by breaking the short again. Then the rotation can be stopped because the charge is now trapped on the condenser. An electrometer measurement shows that the charge indeed exists while its magnitude is of the order given by the off-diagonal term of (74). Pegram performed this experiment to clear up certain questions in the realm of unipolar induction. (See also Kennard 1917.)

This cross relation, between electric and magnetic fields for rotating frames in vacuum, does not occur if one applies the Lorentz-like transformation (29) to describe a rotation. It is not difficult to anticipate this conclusion, because the free-space form of the constitutive tensor (72) is (by definition) invariant for an actual Lorentz transformation. The outcome of Pegram's experiment thus gives further corroborative evidence in favor of transofrmation (11) for the description of rotations.

C. The Wave Equations

Substitution in (71) of the explicit forms (74), (75), (76), and (77) leads to sets of wave equations that apply to the different situations represented by these specific forms of the constitutive tensor. Comparison of the tensor forms [(74) to (77)] shows that they are all of the same form with the Ω-dependent terms occurring in the off-diagonal terms only. To obtain a solution that is also valid in the realm of geometric optical approximations, we start with the assumption that the r and z dependences vanish, which means that we consider a circular beam that is characterized by a ϕ dependence only for a given fixed $r=R$. The substitution of (74) in (71) then leads to the following set of partial differential equations:

$(\lambda=0)$

$$-\frac{\epsilon_0}{R}\frac{\partial^2}{\partial\phi\partial t}A_\phi+\frac{\epsilon_0}{R}\frac{\partial^2}{\partial\phi^2}A_0=0,$$

$(\lambda=1)$

$$R\epsilon_0\frac{\partial^2}{\partial t^2}A_r+2R\Omega\epsilon_0\frac{\partial^2}{\partial\phi\partial t}A_r-\mu_0^{-1}R\frac{\partial^2}{\partial\phi^2}A_r=0,$$

$(\lambda=2)$

$$-\frac{\epsilon_0}{R}\frac{\partial^2}{\partial\phi\partial t}A_0+\frac{\epsilon_0}{R}\frac{\partial^2}{\partial t^2}A_\phi=0,$$

$(\lambda=3)$

$$R\epsilon_0\frac{\partial^2}{\partial t^2}A_z+2R\Omega\epsilon_0\frac{\partial^2}{\partial\phi\partial t}A_z-(\mu_0R)^{-1}\frac{\partial^2}{\partial\phi^2}A_z=0. \tag{78}$$

Inspection of Eqs. (78) shows that the equations for $\lambda=1$ and $\lambda=3$ are identical wave equations in the components A_r and A_s, respectively. The other two equations $\lambda=0$ and $\lambda=2$ are restrictions similar to the Lorentz gauge condition. They relate two remaining components of the four-potential A_ϕ and A_0.

These two equations are dependent because they can be written in the form

$$(\lambda=0)\quad (\partial/\partial\phi)\{(\partial/\partial\phi)A_0-(\partial/\partial t)A_\phi\}=0,$$

$$(\lambda=2)\quad (\partial/\partial t)\{(\partial/\partial\phi)A_0-(\partial/\partial t)A_\phi\}=0. \quad (79)$$

A_0 is the component usually called the scalar potential.

For this simple case we have thus a complete separation of the components and we may therefore consider the single wave equation

$$\epsilon\mu_0(\partial^2/\partial t^2)\psi+2\Omega R\epsilon_0\mu_0(\partial^2\psi/\partial s\partial t)-(\partial^2/\partial s^2)\psi=0, \quad (80)$$

in which ψ can be A_s or A_r. A new coordinate, $s=\phi R$, measures the distance along the periphery of the circle on which the light beams travel.

The wave equation (80) is a vibrating string type of equation except for the nonreciprocal term $2\Omega R\epsilon_0\mu_0\partial^2\psi/\partial s\partial t$. To obtain a solution we may consider the case of the self-oscillating ring laser. The boundary condition corresponding to the self-oscillating case requires that the solutions be single-valued when going around the ring; this means that the circumference of the circle $2\pi R$ should represent an integral number of wavelengths. A substitution of

$$\psi=\exp[i(\omega t+ks)] \quad (81)$$

in Eq. (80) yields

$$\epsilon_0\mu_0\omega^2+2\Omega R\epsilon_0\mu_0\omega k-k^2=0, \quad (82)$$

which is a quadratic equation in ω with solutions

$$\omega_{1,2}=R\Omega k\pm kc[1+(\Omega R/c)^2]^{1/2}. \quad (83)$$

The square root gives a higher-order correction and should therefore be equated to one, because terms of the order $(\Omega r/c)^2$ are already neglected in the evaluation of the transformed constitutive tensor (74). It follows from (83) that the difference between the absolute values of ω_1 and ω_2 becomes

$$\Delta\omega=|\omega_2|-|\omega_1|=2R\Omega k, \quad (84)$$

where the wave number k is the same for the clockwise and counterclockwise modes. For the stationary loop we can write $k=\omega_0/c$ where ω_0 is the single resonant frequency of the stationary loop. The frequency splitting due to the rotation can thus be written

$$\Delta\omega/\omega_0=2R\Omega/c, \quad (85)$$

with $R\Omega=v$, the peripheral velocity of the loop.

Comparison with Eq. (51) for $\alpha=0$, $n=1$, and the beam following a circular path, shows that (51) and (85) lead to identical results.

A similar procedure for the form (76) of the constitutive tensor, which represents the case of a corotating medium, gives for the wave equation

$$\epsilon\mu(\partial^2\psi/\partial t^2)+2\Omega R\epsilon_0\mu(\partial^2\psi/\partial s\partial t)-(\partial^2/\partial s^2)\psi=0. \quad (86)$$

Substituting the solution (81) one obtains the quadratic equation

$$\epsilon\mu\omega^2+2\Omega R\epsilon_0\mu\omega k-k^2=0, \quad (87)$$

which leads to the frequency difference

$$\Delta\omega=2\Omega Rk/\epsilon_r, \quad (88)$$

with ϵ_r the relative permittivity of the medium. Now $k=\omega_0 n/c$, where $n=(\epsilon_r\mu_r)^{1/2}$ is the index of refraction of the medium. Substitution in (88) gives

$$\Delta\omega/\omega_0=2(R\Omega/c)(\mu_r/\epsilon_r)^{1/2}. \quad (89)$$

Comparison with (51), which was obtained by the geometric optical procedure, shows that if we take a circular path of radius R and $\alpha=1-1/n^2$

$$\Delta\omega/\omega_0=2R\Omega/(nc). \quad (90)$$

The equations (89) and (90) become identical if $\mu_r=1$.

The other two possibilities with constitutive forms (75) and (77) are treated in precisely the same manner. For the form (75) the final result agrees excactly with the result obtained from formula (54), which corresponds to a self-oscillating version of the Prunier–Dufour interferometer experiment. The actually observed results have to be corrected for the necessary air gap between the moving mirrors and the stationary medium.

The form (77), mirrors stationary and medium rotating, leads to what may be considered the rotational analog of the translational Fresnel–Fizeau experiment. The results obtained from (77) agree with results obtained from (56) provided $\mu_r=1$. The latter restriction is due to not explicitly accounting for the intrinsic changes in the rotating material.

An electromagnetic analysis of the Sagnac effect was first given by Gordon (1923). His analysis of the free-space case is the exact "wave" counterpart of Langevin's kinematical approach based on the space–time line element. The treatment presented here is mathematically equivalent to Gordon's, but only for the free-space case.

Gordon used a modified metric for the case of a refracting medium in the light beam. This part of Gordon's treatment can only have an *ad hoc* meaning because the ten coefficients of the metric are not adequate to accommodate the maximum of 20 coefficients of the constitutive tensor characterizing a general electromagnetic medium.

Heer (1964) uses a complete set of constitutive relations instead of a modified metric for describing the

properties of a refracting medium in the beam path. No procedure is given for obtaining the constitutive coefficients for the different arrangements of mirror motion and medium motion such as the Dufour-Prunier (1942) arrangement and the rotational analog of the Fresnel-Fizeau experiment.

The electromagnetic procedure presented here was first sketched by Post and Yildiz (1965) and subsequently treated in more detail by Yildiz and Tang (1966).

The final relations for the Sagnac effect are deceptively simple so that one can easily suggest very simple alternatives for obtaining the same first order results. Langevin (1921) had already noted the ambiguity in transformational procedure for obtaining the first-order results (see Sec. III). The significance of the higher-order terms, although experimentally negligible, can be considerable from a theoretical point of view. By also demanding higher-order consistency between comparable kinematical and electromagnetic procedures one may uncover further guidelines for the development of the electromagnetic theory of nonuniformly moving systems.

VI. SUMMARY

The Sagnac effect has been reviewed and discussed against the background of other related optical and mechanical phenomena that can also be used for sensing absolute rotation. In a review of the experimental work on Sagnac-type interferometers, the work of Michelson, Sagnac, Harress, Pogany, Michelson and Gale, and Dufour and Prunier has been discussed in a more or less chronological order. The recent work by Macek and Davis on the self-oscillating version of the Sagnac optical loop, presently known as the ring laser, has also been included.

Alternatives for theoretically analyzing the Sagnac effect have been discussed in Sec. III. The kinematical approach has been applied to the simple model of a circular optical circuit and then carried through in full detail incuding associated higher-order effects when observations are made either in the stationary or in the rotating frame. This analysis has led to a transformation for describing rotations such that the time dilation, which is also an established phenomenon for nonuniform motion, has been properly accounted for. This transformation reduces to an ordinary Galilean rotation if the results are restricted to first orders in the rate of rotation Ω.

A more detailed first-order analysis of Sagnac-type interferometers and ring lasers with optical circuits of arbitrary shape has been presented in Sec. IV. This analysis includes the cases where the light beam travels through a refracting medium. The most prominent experimental arrangements have been discussed quantitatively: medium and interferometer rotating; medium at rest, interferometer rotating; medium rotating, interferometer at rest. Because the principle of relativity does not apply to nonuniform motions, it has been shown that the latter two experiments are different. They would reduce to one and the same experiment (Fresnel-Fizeau) if the motion were a uniform translation.

A completely electromagnetic analysis of the Sagnac effect has been attempted in Sec. V. The application of electromagnetic theory to rotating systems requires some drastic organizational changes of the theory, the most important of which is that the properties of free space are also made explicit in a set of constitutive equations. The constitutive relations on a rotating frame exhibit a cross-coupling between electric and magnetic fields. This cross-coupling is responsible for the occurrence of the Sagnac effect in free space, whereas actual, direct observations of the cross effect have been made by Pegram. The electromagnetic theory in the geometric optical limit leads to exactly the same results as the kinematical approach for all those cases where the material medium is absent or stationary. For the cases where the medium is not stationary one has to take into account the intrinsic changes taking place in the medium as a result of the rotation. The intrinsic change of the medium can be assumed to be negligible for all materials with a relative permeability $\mu_r = 1$. The results of the electromagnetic approach in the geometric optical limit are then in full agreement with the kinematical approach.

ACKNOWLEDGMENTS

The author is indebted to Dr. L. M. Hollingsworth (AFCRL) for many discussions as well as for his help and wise insistence on making a thorough study of the literature.

I had some enlightening discussions with Professor J. G. King and J. Brenner (MIT) on the subject of experimentation on unipolar induction.

D. D. Guidice, P. H. Picard, and F. J. Zucker (AFCRL) are greatfully acknowledged for reading major parts of the manuscript and for their suggestions on how to improve the presentation.

APPENDIX

Consider a Lorentz transformation with a mutual velocity of translation that is arbitrarily oriented with respect to the coordinate axis:

$$t_0 = (t + \mathbf{v}\cdot\mathbf{r}/c^2)\gamma$$

$$\mathbf{r}_0 = \mathbf{r}_0 - \mathbf{v}[(1-\gamma)(\mathbf{v}\cdot\mathbf{r}/v^2) - \gamma t]. \tag{A1}$$

Now consider a rotating disk with two Lorentz frames having a common origin located on the disk's axis of rotation. One frame is taken to be stationary with respect to the disk's axis of rotation while the other

translates with a velocity equal to the instantaneous velocity $\mathbf{v}$ of some point $\mathbf{r}$ of the disk. That point $\mathbf{r}$ then satisfies the equation $\mathbf{v}\cdot\mathbf{r}=0$ as does each point on the disk when related to its own velocity. For the equation $\mathbf{v}\cdot\mathbf{r}=0$ the Lorentz transformation (A1) reduces to

$$t_0=\gamma t$$

$$\mathbf{r}_0=\mathbf{r}+\gamma\mathbf{v}t \tag{A2}$$

and for differentials one has

$$dt_0=\gamma dt$$

$$d\mathbf{r}_0=d\mathbf{r}+\gamma\mathbf{v}dt. \tag{A3}$$

The changes that can be envisioned for a "rigid" rotation obey the relations

$$d|\mathbf{r}|=d|\mathbf{r}_0|=0,$$

$$dr_0=rd\phi_0,$$

$$dr=rd\phi, \tag{A4}$$

with ϕ_0 and ϕ the azimuthal angles and r the radius of the polar coordinates associated with the two frames. If Ω is the rate of angular rotation, the relative velocity v between the two frames is given by

$$v=\Omega r. \tag{A5}$$

A substitution of Eq. (A4) and (A5) in Eq. (A3) yields the infinitesimal transformation

$$dt_0=\gamma dt,$$

$$dr_0=dr,$$

$$d\phi_0=d\phi+\gamma\Omega dt, \tag{A6}$$

which is the same as Eq. (24) if we stipulate that t_0, r_0, and ϕ_0 represent the inertial frame.

The transformation (A6) will, in general, represent a nonintegrable relation between the differentials of the coordinates. This nonintegrability or anholonomity stems from the requirements of rigidity (A4).

To obtain the inverse transformation one solves (A6). Then

$$dt=\gamma^{-1}dt_0,$$

$$dr=dr_0,$$

$$d\phi=d\phi_0-\gamma\Omega dt,$$

$$=d\phi_0-\Omega dt_0.$$

Notice that this result, unlike that of the Lorentz transformation, cannot be obtained by a simple inversion of the velocity sign. In fact the position of the factors γ in (A6) and (A7) allows us to distinguish between transformations from an inertial to a rotating frame and vice versa.

A comparison of (A6) and (A7) shows that there is a difference $\Delta\Omega$ between the rates of rotation as observed in the inertial and rotating frames.

$$\Delta\Omega=(\gamma-1)\Omega. \tag{A8}$$

This difference corresponds to a change in time "measure" associated with a "centrifugal" potential, similarly as the change in time "measure" that is associated with a gravitational potential.

Equation (A8) gives the Thomas precession for a circular path.

BIBLIOGRAPHY

Barnett, S. J., 1915, Phys. Rev. 6, 239.
Brandstatter, J. J., 1963, *Waves, Rays and Radiation in Plasmas* (McGraw-Hill Book Co., Inc., New York), p. 272.
Cartan, E., 1924, Ann. Ec. Norm. 41, 1.
Dorgelo, H., and Schouten, J. A., 1946, Proc. Amsterdam Acad. 40, 124, 282, 394.
Dufour, A., and Prunier, F., 1937, Compt. Rend. 204, 1322.
——, and Prunier, F., 1942, J. Phys. Radium, 8th Ser. 3, 153.
Einstein, A., 1914, Astron. Nachr. 199, 9 and 47.
Fock, V., 1959, *The Theory of Space, Time and Gravitation* (Pergamon Press, Inc., New York).
Gordon, W., 1923 Ann. Physik 22, 421.
Harress, F. 1911, thesis, Jena (unpublished).
Harzer, P., 1914, Astron. Nachr. 198, 378.
——, 1914, Astron. Nachr. 199, 10.
Heer, C. V., 1964, Phys Rev. 134A, 799.
Kennard, E. H., 1917, Phil. Mag. 33, 179.
Kromykh, A. T., 1966, Zh. Eksperim. i Teor. Fiz. 50, 281 [English transl.: Soviet Phys.—JETP 23, 185 (1966)].
Langevin, P., 1921, Compt. Rend. 173, 831.
——, (1937), Compt. Rend. 205, 51.
Macek, W., and Davis, D., 1963, Appl. Phys. Letters 2, 67. [For a recent review of ring laser work plus a bibliography on ring lasers see W. M. Macek and E. J. McCartney, Sperry Eng. Rev. 19, 8 (1966).]
Madelung, E., 1943, *Mathematical Tools for the Physicist* (Springer-Verlag, Berlin), p. 129.
Metz, A., 1952, J. Phys. Radium 13, 224.
——, 1952, Compt. Rend. 234, 597.
——, 1952, Compt. Rend. 234, 705.
Michelson, A. A., and Morley, E. W., 1886, Am. J. Sci. 31.
——, and Morley, E. W., 1887, Am. J. Sci., 3rd Ser. 34, 333.
——, and Morley, E. W., 1887, Phil. Mag. 24, 449.
——, 1897, Am. J. Sci., 4th Ser. 18, 475.
——, and Gale, H. G., 1925, Nature 115, 566.
——, and Gale, H. G., 1925, Astrophys. J. 61, 137.
Pegram, G. B., 1917, Phys. Rev. 10, 591.
Poeverlein, H., 1962, Phys. Rev. 128, 956.
Pogany, B , 1926, Ann. Physik 80, 217.
——, 1928, Ann. Physik 85, 244.
Post, E. J., 1962, *Formal Structure of Electromagnetics* (North-Holland Publ. Co., Amsterdam).
——, and Yildiz, A., 1965, Phys. Rev. Letters 15, 177.
Rosenthal, A. H., 1962, J. Opt. Soc. Am. 52, 1143.
Sagnac, G., 1913, Compt. Rend. 157, 708, 1410.
——, 1914, J. Phys. Radium, 5th Ser. 4, 177.
Schiff, L. I. 1939, Proc. Natl. Acad. Sci. U.S. 25, 391.
Trocheris, M. G., 1949, Phil. Mag. 40, 1143.
Van Dantzig, D., 1934, Proc. Cambridge Phil. Soc. 30, 421.
——, 1934, Proc. Amsterdam Acad. 37, 521, 526, 644, 825.
von Laue, M., 1920, Ann. Phys. 62, 448.
Weyl, H., 1951, *Space-Time-Matter* (Dover Publication, Inc., New York).
Yildiz, A., and Tang, C. H., 1966, Phys. Rev. 146, 947.
Zernike, F., 1947, Physica 13, 279.

APPENDIX B

RNAL OF THE OPTICAL SOCIETY OF AMERICA VOLUME 52, NUMBER 10 OCTOBER 1962

Regenerative Circulatory Multiple-Beam Interferometry for the Study of Light-Propagation Effects

ADOLPH H. ROSENTHAL*
Kollsman Instrument Corporation, Elmhurst, New York
(Received October 10, 1961)

Novel circulatory and regenerative multiple-beam interferometry methods making use of optical maser oscillations of extreme monochromaticity based on stimulated emission present interesting possibilities for investigating with high-precision various effects of motion and of fields on the propagation of light. These methods inherently permit increasing considerably the accuracy of the historical relativistic experiments of Michelson, Sagnac, and others, and have also potential applications to studies of other radiation propagation effects in magnetic, electric, and gravitational fields, and in moving refractive media, and to the modulation of coherent radiation. These propagation effects can produce frequency splits of the optical-maser oscillations, and the frequencies of the resulting optical beats are a measure for those effects; frequency measurements can be accomplished with high accuracy by using primary frequency standards, e.g., atomic clocks. Contrary to the many proposed applications of optical masers which are directed towards utilizing the high spatial coherence of the wave fields, the present subject is thus primarily concerned with the narrow-frequency bandwidths possible with these novel radiation sources. The high accuracies possible with the new interferometric methods described should lead to quantitative results which up to now were either impossible to achieve, or only by experiments on very large scales.

I. INTRODUCTION

IN the classical experiments of Michelson, Sagnac (illustrated in Figs. 1 and 2) and others[1–5] to study the effect of the rotation of a system on light propagation within that system, the interpretation of which has been closely linked to the theories of relativity,[6–9] a modified *Michelson two-beam interferometer* is used in which light from a source is split by a beam-splitter into two coherent beams which, by suitably arranged mirrors, are made to travel around a closed circuit in opposite direction but along identical paths, and then are combined again at the beam-splitter and brought to interference. The rotation of the system produces a fringe shift Δp (measured in fringe numbers) as a result of differential path changes for the clockwise and counterclockwise beams:

$$\Delta p = 4\omega S \cos\varphi/c\lambda, \qquad (1)$$

where ω is the angular velocity, S the area of the optical circuit, φ the angle between the normal to the plane of the circuit and the rotation axis, λ the wavelength, and c the light velocity.

If the rotation is, for instance, that of the earth around its axis ($\omega = 7.27\times10^{-5}$ rad/sec), the fringe shift at 40° latitude for a horizontal square circuit of 3-m side length, i.e., an area of 9m², for $\lambda = 5\,000$ Å would amount, according to Eq. (1), to just over 10^{-5}. The observation of such small fringe displacements becomes very difficult with the standard two-beam interferometric methods, and Michelson and Gale[3] in their 1925 experiment had to use an optical circuit of an area of over 200 000 m² to obtain a fringe shift of less than $\frac{1}{4}$.

II. CIRCULATORY MULTIPLE-BEAM INTERFEROMETERS

The intensity curve of the interference fringes for monochromatic light in such a Michelson type two-beam interferometer has a $\cos^2$ shape, which makes the half-intensity width of the fringes equal to half their spacing. This seriously limits the spectral resolving power as well as the possibility of measuring such small fringe shifts.

Interference fringes resulting from a multiplicity of interfering beams become increasingly sharp as the number of interfering beams increases and their half-width may amount then to only a small fraction of their spacing.[10] Such multiple-beam interferences form the basis of high-resolution spectroscopes, e.g., Fabry-Perot interferometers, and also of diffraction gratings.

To apply multiple-beam interferometry to the evaluation of very small fringe shifts Δp, it is necessary, first, to reduce the "monochromatic" instrument half-intensity fringe width W (expressed as a fraction of the distance of adjacent fringes) below the fringe shift to be measured. Secondly, the light source used must be sufficiently monochromatic, i.e., it must have a linewidth below that instrument width.

The first condition would require $W \approx 1/N_e \leq k\Delta p$, where $1/k$ is a still measurable fraction of the fringe width (for refined half-shadow photoelectric methods, k may amount to several thousand[11,12]), and N_e is the effective number of interfering beams. In interferometers

* Died July 21, 1962.
[1] A. A. Michelson, Phil. Mag. 8, 716 (1904).
[2] G. Sagnac, J. phys. radium 4, 177 (1914).
[3] A. A. Michelson and H. G. Gale, Nature 115, 566 (1925); Astrophys. J. 61, 137, 140 (1925).
[4] F. Harress, Diss. Jena (1911).
[5] B. Pogany, Ann. Physik 80, 217 (1926).
[6] L. Silberstein, J. Opt. Soc. Am. 5, 291 (1921).
[7] M. von Laue, Ann. Physik 62, 448 (1920).
[8] H. Witte, Verhandl. deut. physik. Ges. 16, 143, 754 (1914).
[9] C. Runge, Naturwissenschaften 13, 440 (1925).
[10] See for instance, S. Tolansky, *An Introduction to Interferometry* (Longman's Green and Company, Inc., New York, 1955) p. 118–127.
[11] R. J. Kennedy, Proc. Natl. Acad. Sci. U. S. 12, 621 (1926).
[12] K. K. Illingworth, Phys. Rev. 30, 692 (1927).

TABLE I. Monochromatic light sources used or proposed as metric standards.

Source	$\Delta\lambda/\lambda$
(1) Cadmium 6438 Å	1.75×10^{-8}
(2) Krypton (86) 6058 Å	7.3×10^{-9}
(3) Calcium 4226 Å (atomic beam)	1.27×10^{-7}

where the multiple beams result, like in a Fabry-Perot, from repeated reflections by mirrors, N_e increases with the mirror reflectance R: $N_e=\pi R^{\frac{1}{2}}/(1-R)$, and values of many hundreds can be easily obtained; for instance, with multilayer dielectric reflectors, reflectance values of over 99.5% can be achieved for narrow spectral bands, resulting in N_e values of about 580.

The second condition would require for the relative source linewidth $\Delta\lambda/\lambda\leq 1/pN_e$, where p is the path difference, in wavelengths, between consecutive interfering beams. In the above example of a square-shaped Michelson-Sagnac circuit of 3-m side length, this path difference, equal to the circumference of the circuit, is 2.4×10^{7} for $\lambda=5\,000$ Å, and assuming $N_e=100$, the relative source linewidth $\Delta\lambda/\lambda$ would have to be smaller than 4×10^{-10}.

The best monochromatic light sources available until recently and used or proposed as metric standards[13] have relative linewidths $\Delta\lambda/\lambda$ of over 10^{-7}, far in excess of this requirement, as shown in the Table I.

The narrowest line of this table, the 4226 Å calcium line, obtained by Meissner from an atomic beam source,[14] still has a relative linewidth $\Delta\lambda/\lambda$ of over 10^{-7}.

The product pN_e which enters the second condition represents the resolving power of the interferometer, and is synonymous with its resonator quality factor Q.

Recent developments of optical-maser light sources based on stimulated emission have made it possible to obtain monochromaticity values better by several orders of magnitude.[15] A relative linewidth of down to about 10^{-14} has already been realized in the stimulated emission of the 11 530 Å neon line in a neon-helium gas-discharge optical maser, with a frequency bandwidth of this line of less than 2 cps.[16,17]

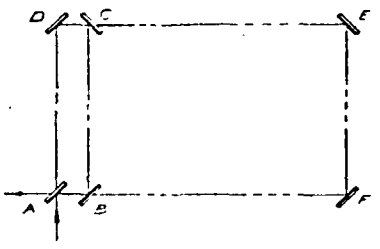

FIG. 1. Two-beam interferometer arrangement used in the experiment of Michelson and Gale.

To utilize the high-monochromaticity values of these new light sources to the fullest extent in an interferometer of the Michelson-Sagnac type, it is necessary to maintain the highest instrument resolution and, therefore, number of interfering beams in the interferometer.

In the historical experiments shown in Figs. 1 and 2, the optical circuits for the clockwise and counterclockwise beams contain a beam splitter with a transmission and reflection coefficient of about 50%. Therefore, even if one would return the light to the circuits by placing a mirror of a high-reflecting power into the incoming or outgoing beam, the beam splitter would prevent any effective multiple-beam formation as well as multiple traverses. It is necessary to isolate the optical circuits as much as possible from the beam splitter, and to retain a maximum of the circulating light flux within the circuit.

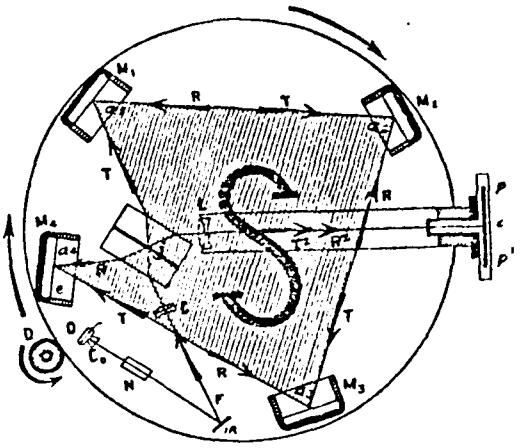

FIG. 2. Two-beam interferometer arrangement with light source and camera on turntable used in the experiment of Sagnac.

Figure 3(a) exemplifies an interferometer configuration which would meet this requirement. The main optical circuit determined by the mirrors A, B, C, D encloses the area S which enters in Eq. (1). Mirrors B, C, D are totally reflecting; mirror A should have a high-reflecting power R of 95% to 99%, transmitting only a small percentage of the light. An auxiliary, usually much smaller optical circuit, is formed by the mirrors A, E, F, G, of which E and F are totally reflecting, and G, the beam splitter, is about 50% reflecting and 50% transmitting. The optical maser, acting here as the outside light source, includes the active medium M, capable of being excited to stimulated optical emission—the energy source to produce the population inversion is not shown—and placed within a suitable resonance cavity consisting, e.g., of a Fabry-Perot interferometer formed

[13] Comite International des Poids et Mesures, Paris (1960).
[14] K. W. Meissner and V. Kaufman, J. Opt. Soc. Am. 49, 434, 942 (1959).
[15] A. L. Schawlow and H. C. Townes, Phys. Rev. 29, 1940 (1958); A. L. Schawlow, *Quantum Electronics* (Columbia University Press, New York, 1960) p. 553.
[16] A. Javan, W. R. Bennett, Jr., and D. R. Herriott, Phys. Rev. Letters 6, 106 (1961).
[17] A. Javan, E. A. Ballik, and W. L. Bond, J. Opt. Soc. Am. 52, 96 (1962).

by the totally reflecting mirror I and the highly reflecting mirror H, from which the coherent light emerges towards the beam splitter G where it is divided into the clockwise and counterclockwise beams. These enter the main circuit A, B, C, D at A, and, as a consequence of its small losses, can traverse this circuit a multiple number of times, coming to interference again at A. Part of this returning light will then be directed by a lens system L into a photoelectric transducer P, which may consist of a double photoelectric cell system in a suitable bridge circuitry, using a sensitive split-field method with which small fractions of a fringe shift can be measured. In this configuration also a Mach-Zehnder type interferometer arrangement might be used, with two separate auxiliary circuits, at the opposite ends of a diagonal of the main circuit, for the light input and output.

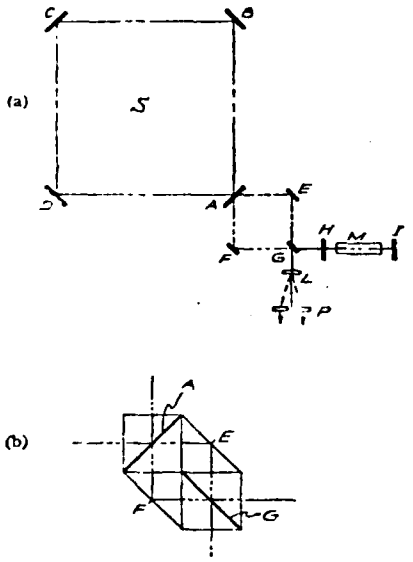

FIG. 3. (a) Schematic of circulatory multiple-beam interferometer with optical maser as outside light source. The resolution is instrument limited. (b) Prism assembly for auxiliary circuit of Fig. 3.

Figure 3(b) shows an assembly of cemented prisms for the auxiliary circuit A, E, F, G, forming a self-contained stable unit. The prism surfaces A and G carry the reflecting surfaces with the 95% to 99%, and 50% reflectance, respectively, which can be made up by multilayer dielectric films.

In this interferometer the interfering light beams circulate an integer number of times around the circuit, whereas in a Fabry-Perot etalon they travel forth and back between the two parallel end plates. The path difference p of two consecutive interfering beams which, in a Fabry-Perot, is twice the distance between the end plates, is here equal to the circumference of the circuits, i.e., $4l$ for a square with sides l.

With a 1-m-square interferometer of the type shown in Fig. 3, assuming for mirror A a reflectance of 99.5%,

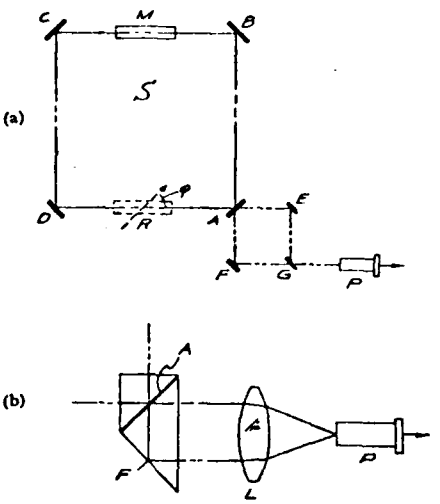

FIG. 4. (a) Schematic of regenerative circulatory multiple-beam interferometer with optical maser forming a part of the main interferometer circuit. The resolution is source limited. (b) Prism arrangement for auxiliary output circuit.

and with a photoelectric split-field transducer system of a sensitivity $1/k$ of 1/1000 fringe, the terrestrial rotation would be easily measurable.

The resolution of the interferometer configuration of Fig. 3, however, is still instrument limited and does not make the fullest use of the high-monochromaticity values of optical maser sources.

III. REGENERATIVE CIRCULAR MULTIPLE-BEAM INTERFEROMETERS

To utilize fully the high monochromaticity values already available from optical maser sources, and obtain the highest spectral resolution, only limited by the source, other interferometer configurations have been devised. In these configurations the optical maser light source forms an integral part of the interferometer circuit, as illustrated in Figs. 4(a, b) where again M indicates the active medium capable of being excited to stimulated emission [Fig. 4(b) shows a prismatic arrangement corresponding to that of Fig. 3(a)].

The circumferential circuit path p defined by mirrors A, B, C, D which, except mirror A, are totally reflecting, now represents the resonance cavity. Mirror A with a reflectance of, say 99.5%, permits the radiation to leave the circuit.

This configuration constitutes a regenerative circulatory multiple-beam interferometer which permits the development of a very high effective number N_e of interfering beams as a consequence of the regenerative maser action and of the high-reflectance values maintained throughout the circuit, resulting in a high-circulation rate of the clockwise and counterclockwise light beams.

The stimulated emission of the active medium M of the optical maser contained within and forming part of the interferometer cavity compensates for the losses at

the mirrors caused by reflection and diffraction, resulting in a very large increase in the spectral-resolving power, i.e., the effective Q of the cavity.

Contrary to conventional optical-maser configurations where the cavity and oscillation modes are essentially defined by the end reflectors, whether plane or spherical, in these circulatory optical-maser configurations the oscillation modes are determined by the phase relationship in the closed optical circuit, i.e., by its optical circumference.

IV. FREQUENCY SPLIT AND OPTICAL BEATS

The circumferential optical path p of the circuit constituting the essential cavity dimension, determines the frequency ν of the preferred mode resonance (s) (within the linewidth of the spontaneous emission) of the maser oscillation. Therefore, in experiments of the Michelson–Sagnac type, the slight difference in the circumferential optical paths for the clockwise and counterclockwise beams, as a consequence of the rotation of the system, will result in a lifting of the degeneracy, i.e., in a frequency split $\Delta\nu$ between oppositely circulating modes. With Eq. (1) one obtains with good approximation, (neglecting the different refractive index of the active medium)

$$\Delta\nu = \nu\Delta p/p = (\omega l \cos\varphi)/\lambda \qquad (2)$$

for a square-shaped circuit with sides l.

Combining the highly coherent oppositely circulating beams as indicated in Figs. 4(a,b) by means of auxiliary mirrors E, F, G and/or lens L in a photoelectric transducer P, will produce a corresponding beat frequency $\Delta\nu$ which can be measured with great precision, for instance, by electronic superheterodyne methods.[18] The accuracy of frequency measurements, e.g., by comparison with primary frequency standards such as atomic clocks, can be better than one part in 10^{11}.[19]

Simultaneous oscillation of two axial modes at discreet frequencies within the natural (radiative) linewidth, drawing on different supplies of atoms, has been recently observed by Javan, and can occur particularly if the gain in the active medium sufficiently surpasses the threshold value[20]; it could in any case be enforced by placing a plane transparent surface of small reflectance within the circuit, perpendicularly to the beam propagation, for instance, between mirrors A and D.[21]

The frequency bandwidth of the maser oscillations determines the minimum measurable beat frequency, i.e., resolution or sensitivity of the measurements, for instance, in the case of Michelson–Sagnac type experiments, the minimum measurable angular velocity, or the minimum size, of the optical circuit. According to Eq. (2), the terrestrial rotation of a 1-m-square horizontal circuit at 40° latitude, using the above-mentioned 11 530 Å neon line, would produce, for instance, a frequency split or beat frequency of about 40 cps; with such a circuit on a platform rotating at 1 rpm a frequency split or beat frequency of about 9 kc would result. In both cases the frequency split, or the beat frequency, is considerably larger than the optical maser frequency bandwidth (of a few cycles).[16,17]

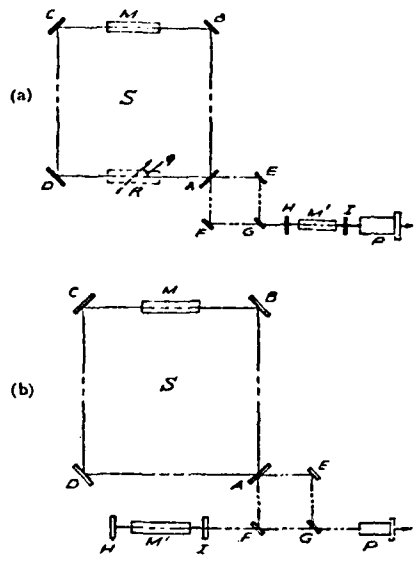

FIG. 5. Schematics of two alternative arrangements of regenerative circulatory multiple-beam interferometers for photoelectric mixing of the outputs of the two optical masers, one forming a part of the main interferometer circuit, the other one outside the circuit.

Even for frequency splits smaller than the bandwidth of the maser oscillations, the modified line shape, and thereby the frequency split, can be determined by optical superheterodyne methods, for instance, by mixing with the output of a second optical maser M′ outside the optical circuit (in its Fabry-Perot interferometer cavity H-I), as indicated in Figs. 5(a,b).

These configurations of Figs. 5(a,b), containing a separate comparison oscillator outside of the optical circuit which is, therefore, unaffected in its frequency by the rotational effects, would provide a sensitive tool to measure such rotational (and related) effects, even if through low gain, or otherwise, both oppositely circulating modes would not oscillate simultaneously within the regenerative circuit.

V. RECOIL-FREE GAMMA RAY SOURCES

Since the fringe shift in the Michelson–Sagnac experiment [Eq. (1)], and the beat frequency [Eq. (2)], are inversely proportional to the wavelength λ, the use of x or γ rays would appear to imply higher sensitivity.

[18] A. T. Forrester, J. Opt. Soc. Am., 51, 253 (1961).

[19] R. C. Mockler, R. E. Behler, and C. S. Snider, I.R.E. Trans. on Instrumentation, I-9, 120 (1960).

[20] See reference 17, and private communication by Dr. A. L. Schawlow.

[21] Dr. A. L. Schawlow kindly pointed out to the author that also the possibility exists here of applying a fixed magnetic field large enough to separate two Zeeman components by more than the natural linewidth. If this field is arranged parallel to the beam direction, the two circularly polarized components could be excited by the clockwise and counterclockwise beams, respectively.

The construction of suitable interferometers would be, however, quite difficult in this region mainly in view of the extremely small coherence length of these radiations.

The recoil-free γ-ray radiation effects discovered by Mössbauer[22] for the first time made available in this region monochromaticity values of the same order of magnitude as those obtainable from optical-maser sources. This indicates the possibility, at least in principle, of utilizing also these short wavelength radiations in measurements of this kind.

VI. POTENTIAL APPLICATIONS TO VARIOUS REFRACTOMETRIC MEASUREMENTS AND TO MODULATION

The rotational frequency split described in the previous Sec. IV resulting from the difference in the effective cavity resonance dimensions for the clockwise and counterclockwise light beams, may, viewed from the rotating system, also be regarded as a consequence of an effective difference of the refractive indices for these two beams in the interferometer cavity space. From this point of view, the rotational effect on the propagation of radiation introduces a directional anisotropy, i.e., a kind of birefringence in the interferometer circuit. The interferometer circuit in this respect acts actually as a sensitive refractometer.

These regenerative interferometers represent, therefore, a new tool for various investigations and measurements which can be related to refractive-index changes, and to various kinds of birefringence, and may also include effects of pressure, temperature, chemical changes, motion, etc., upon the refractive index of a medium enclosed within the interferometer cavity. They have also potential applications to the modulation of coherent radiation.

Such investigations can be based on natural birefringence, including optical activity, of crystals and other substances, photo-elasticity, or birefringence caused by various fields, e.g., of magnetic, electric, or gravitational origin.

Generally, any birefringence resulting in a difference Δn in the refractive indices will cause a frequency split or beat frequency, which, from Eq. (2) is

$$\Delta\nu=\nu\Delta p/p\approx\nu\Delta n p_R/p, \tag{3}$$

where p is the path difference of the interferometer cavity, and p_R the part thereof over which the birefringence occurs, indicated in Figs. 4 and 5 by a region R.

This beat-frequency method permits the measurement of quite small birefringences. It follows, for instance, from Eq. (3) that with an interferometer path p of 100 cm, the natural birefringence of a 10-μ-thick calcite crystal would give a frequency split of about 10^3 cps; the (rotary) optical activity of a 10μ-thick quartz crystal would give a frequency split of about 300 kc, and an average photoelastic material, 1-cm thick, would produce a frequency split or beat frequency of several kc, if subjected to a pressure of 10g/cm^2(for Na D light).

In magnetic field investigations the Faraday-effect birefringence for oppositely circularly polarized light can be utilized. If the magnetic field, indicated by an arrow in Figs. 4 and 5, forms an angle φ with the radiation direction AD, the difference in refractive indices for right and left circularly polarized light is

$$\Delta n=n_r-n_l=(2/\pi)VH\cos\varphi, \tag{4}$$

where H is the magnetic field strength and V the Verdet constant. If H is measured in gauss, and V in min/G cm, this difference becomes approximately

$$\Delta n=n_r-n_l\approx 9.2\times10^{-5}\lambda VH\cos\varphi \text{ cps}. \tag{4a}$$

This birefringence will cause, with Eq. (3) and (4a), a frequency split of

$$\Delta\nu\approx 2.8\times10^6 VHp_R/p\cos\varphi \text{ cps}. \tag{4b}$$

If we assume that this Faraday-effect birefringence extends over $\frac{1}{10}$ of the interferometer path, and, since for most transparent solids and liquids, V is of the order of 10^{-2}, and for gases around 10^{-5}, this beat frequency will amount for solids and liquids to about $3\times10^3 H\cos\varphi$ cps, and for gases to about $3H\cos\varphi$ cps.

The example of magnetic-field investigations based upon the Faraday effect has been described in some detail. Other field-effect measurements, for instance, based on the Cotton-Mouton magneto-optic effect, which is predominant if the field is perpendicular to the light propagation and which results in a birefringence of light polarized parallel and perpendicular to the field, can also be utilized. Generally, both these magnetic field effects are present. Also the magneto-optic Voigt effect near absorption lines, and the magneto-optic Kerr effect occurring when light is reflected at ferromagnetic mirrors might be considered.

Similarly to the effects of magnetic fields, those of electric fields can be utilized for investigations by the above described interferometric methods. Electric fields produce electro-optic birefringence, either if the field is perpendicular to the propagation of the radiation—the Kerr electro-optic effect exhibited by many liquids, or, if the field is parallel to the radiation—the Pockels effect exhibited by many crystalline substances, such as Sphalerite, or synthetics such as ADP, KDP.

In the electro-optic Kerr effect the transverse electric field E produces a difference of the refractive indices for light which is polarized parallel or perpendicular to the field:

$$\Delta n=n_{||}-n_{\perp}=\lambda BE^2. \tag{5}$$

Nitrobenzene has the largest known Kerr constant, $B=4.6\times10^{-10}$ (where E is in V/cm).

With Eqs. (3) and (5) a frequency split will result, amounting to

$$\Delta\nu=13.8p_R/pE^2 \text{ cps}. \tag{5a}$$

[22] R. L. Mössbauer, Z. Physik 151, 124 (1958); Naturwissenschaften 45, 538 (1958). Z. Naturforsch. 14a, 211 (1959).

Thus, with an interferometer path of 100 cm and a Kerr-effect region of 10 cm

$$\Delta\nu = 1.38E^2 \text{ cps.} \tag{5b}$$

This amounts, for a field of 1000 V/cm, to a frequency split of 1.38 Mc, and for a field of 150 kV/cm, which is near the breakdown field, to a frequency split of 3.1×10^{10} cps (corresponding to a modulation wave length of less than 1 cm).

In some of these field effects (the longitudinal ones) the difference in the refractive indices and therefore the frequency split is proportional to the field strength (Faraday and Pockels effects), and in others (the transverse ones) to the square of the field strength (Cotton–Mouton and electro-optic Kerr effects).

It is interesting to note, from Eq. (3), that these frequency splits, and thus beat frequencies, depend essentially only upon the ratio between the length p_R of the optical-path region subjected to the field and the total optical path p of the interferometer cavity, but are independent of the absolute dimension of the interferometer.

These effects could, in principle, also be investigated with a standard parallel mirror Fabry–Perot arrangement including an active optical-maser medium in a part of the space between its mirrors. Any changes in the refractive index occurring in other regions of the cavity will cause a change in the cavity resonance, and therefore, in the frequency of the stimulated emissions. Magnetic and electric fields act also directly upon the atomic levels of the active optical-maser medium, e.g., in the Zeeman and Stark effects, respectively. An advantage of the circulatory regenerative multiple-beam interferometer configurations over a straight Fabry–Perot arrangement for the investigation of such field effects is the ease with which the region of the field action can be separated from that of the active medium. For instance, as shown in Figs. 4 and 5, the medium subjected to the fields can be placed in the region R between mirrors A and D, separated and shielded from the active medium M.

The wide range of frequency splits and beat frequencies obtainable from the various birefringence effects represents a flexible means for modulating the optical-maser oscillations, which, particularly in the case of the field birefringences, are thereby readily controllable over a wide range of modulation frequencies.

Another interesting application of these regenerative circulatory multiple-beam interferometers concerns measurements of light propagation in moving refractive media. If, for example, a liquid with refractive index n flows through a container as indicated at R in Figs. 4 and 5 with a velocity v in the direction of one of the circulating light beams, the light velocities of the two beams in the moving medium are, according to Lorentz's formula

$$U_{1,2} = \frac{c}{n} \pm v\left(1 - \frac{1}{n^2} - \frac{\lambda}{n}\frac{dn}{d\lambda}\right). \tag{6}$$

For $v<c$, and neglecting the dispersive term, this results in a change of the refractive index for each beam, as a consequence of the motion, of

$$\Delta n_{1,2} = \pm(V/c)(n^2-1). \tag{7}$$

The corresponding frequency change is from Eq. (3)

$$\Delta\nu_{1,2} = \pm\nu p_R/p\,\frac{v}{c}(n^2-1) \text{ cps.} \tag{8}$$

The two oppositely circulating beams will thus produce a beat frequency

$$\Delta\nu = 2\nu p_R/p\,\frac{v}{c}(n^2-1) \text{ cps.} \tag{9}$$

If we assume again a value of $\frac{1}{10}$ for p_R/p, and water with $n=1.33$ as the moving medium, the beat frequency for a wavelength of 1 μ is

$$\Delta_p = 1.56\times10^3 v \text{ cps} \tag{9a}$$

A flow velocity of 1 cm/sec will then produce a beat frequency of about 1500 cps.

Other radiation effects, for instance, from gravitation and acceleration fields and from space anisotropies of mass distribution, and also second-order velocity effects, usually require for their investigation—as did the original Michelson–Gale experiment—optical instrumentation on quite a large scale. By relating such effects to apparent refractive index changes in the interferometer cavity space, they might be quantitatively investigated with regenerative interferometer configurations of moderate size.

APPENDIX C

Progress on laser gyros stimulates new interest

By Howard Greenstein

DEVELOPMENT of the ring-laser gyroscope represents a revival of interest in optical rotation sensing nearly half a century after the technique had been abandoned for lack of coherent light sources. The promise of laser-gyro research is a purely optoelectronic rotation sensor, with no moving parts. The prospective commercial importance of laser-based angular-position and -rate sensors, for applications in navigation, guidance and flight-control systems, has prompted an increasing number of avionics systems manufacturers to initiate in-house laser-gyro programs.

A prominent role seems assured in future avionics systems, but cost-effective versions remain to be developed

The significance of a nonmechanical rotation sensor is twofold. First, the absence of a spinning mass provides immunity to a variety of mechanical effects that limit the performance of mechanical gyroscopes. Second, the concept of the laser gyro is so simple and elegant that it offers the prospect of a lowcost, rugged and highly reliable rotation sensor. Although these advantages have not all been realized, laser-gyro development has reached the stage where the instrument's credibility is now well established.

The development period has been longer than first anticipated, but mechanical-gyro technology also was slow to develop and did not attain maturity until the 1950s and 1960s, when a remarkable series of engineering achievements opened the way to substantial reductions in price and improvements in reliability. Since mechanical-gyro development appears to have passed the point of diminishing returns, attention has turned to unconventional rotation sensors, of which the laser gyro remains the most promising.

The laser gyro has demonstrated its ability to avoid the mechanical limitations of wheel gyros, which include dynamic errors that vary with linear velocity and linear acceleration, and loss of accuracy for rotation rates faster than about 10 revolutions per minute. In contrast, the laser gyro is insensitive to linear-motion effects and can easily accommodate high angular rates. It also is immune to cross-coupling errors that degrade performance in mechanical gyros because of multi-axis sensitivity.

Additional attractions include an output that appears naturally in digital form, rapid response — typically in microseconds — to a sudden maneuver, dynamic range up to eight decades, and fast warm-up. Some of these features clearly are of general interest, but others have more specific utility. For example, laser gyros function well in missile-guidance applications, whereas mechanical gyros exhibit both g and g^2 errors in a high-stress environment.

The operational features that make the laser gyro unique have been largely (although not entirely) verified, but the prospective cost advantage has yet to materialize. So far this question has received relatively little attention, however because laser-gyro development has been concerned primarily with reliability and accuracy.

With respect to the latter specification it is natural to assess laser gyros against the accuracy standards that have been established by mechanical gyros. In a sense, one of the problems in laser-gyro development has been the fact that these standards are extraordinary. For example, high-performance mechanical gyros exhibit random-drift rates less than 0.001 degree per hour — one revolution in 40 years! For laser gyros the current state of the art is defined by an effective drift rate slightly below 0.01 degree per hour. In navigational applications this translates roughly into an error rate of one nautical mile per hour, which is the minimum requirement to qualify as an "intertial-grade" sensor — that is, one acceptable for use in inertial-navigation systems.

Precision inertial-navigation systems require inertial sensors of the highest accuracy (within 0.01 to 0.001 degree per hour). However there are many other applications where the requirements are much less severe, including aided inertial-navigation systems (which receive periodic updates from radio or other ground-based sources), attitude- and heading-reference systems, and missile- and space-guidance systems. Here the laser gyro can provide the requisite accuracy, between 0.01 and 10 degrees per hour, although it is still not cost-competitive.

Inertial-grade accuracy does not represent the ultimate theoretical limit for the laser gyro. High accuracy is difficult to achieve because a practical design must offer a solution to the lock-in problem described below; with currently favored solutions

Howard Greenstein is visiting scholar at Stanford University. He holds a bachelor of science (summa cum laude) from Brown University and a doctorate in physics from Stanford and has conducted research on novel methods of ring-laser-gryo operation.

control of residual error sources imposes severe constraints in design and construction that compromise the simplicity and cost-effectiveness of the original concept. Although further development presumably will lead to improvements in conventional techniques, the elegance of the basic method will continue to invite novel solutions, and current research is proceeding down both new and old paths.

Detecting path-length differences

In general, optical rotation sensors function by detecting a differential shift in optical-path length between two beams propagating in opposite directions around a closed path. The original method was the sagnac interferometer,[1] in which a beam-splitter divided an incident beam so one component beam traversed the perimeter of a rectangle in a clockwise direction and the other in a counterclockwise direction prior to recombination. The rotation induces a fringe shift in the interference pattern proportional to rotation rate. In practice the sagnac device is limited in sensitivity; to detect the 15-degree-per-hour rotation of the earth about its axis A.A. Michelson and H. G. Gale[2] in 1925 had to extend the interferometer dimensions to about half a kilometer.

The Michelson-Gale experiment marked both the zenith and terminus of this early activity, although interest in the sagnac-type sensor has recently been revived. To take things in historical order, however, the renaissance of optical rotation sensors dates from 1962, when A.H. Rosenthal[3] proposed a configuration whose high sensitivity would be derived from

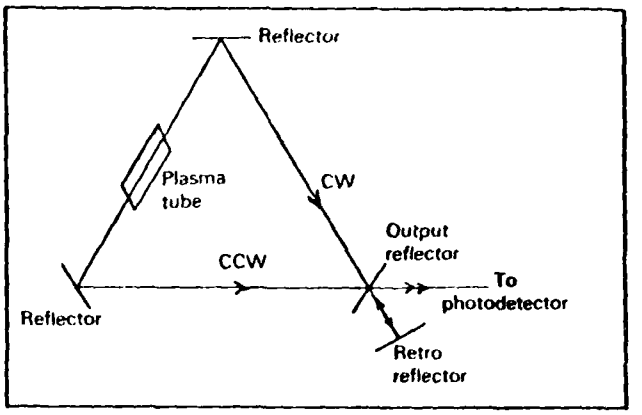

Fig 1 *Configuration of a triangular ring-laser gyro*

the extraordinary coherence properties of laser radiation. This is accomplished by combining the optical-generation and rotation-sensing functions in a laser oscillator with a ring-shaped cavity — typically a square or a triangle, as shown in Fig. 1. Rotation then induces a difference in the generation frequencies for the two traveling waves that propagate in opposite directions around the ring.

The frequency split Δf is proportional to rotation rate Ω, in principle according to the relationship

$$\Delta f = \frac{4A}{\lambda p}\,\Omega \qquad (1)$$

where A and p are the area and perimeter of the ring, and λ is the wavelength of oscillation. For a typical laser gyro, with a ring area on the order of

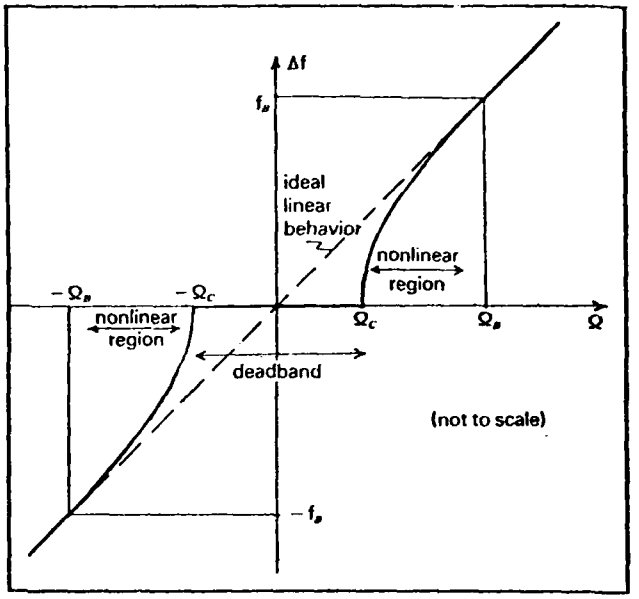

Fig 2 *Observed laser-gyro response with difference frequency Δf plotted against rotation rate Ω, showing the lock-in and nonlinear effects. An artificially induced equivalent rotational input Ω_B gives rise to the bias frequency f_B. With a periodic bias and a stationary laser gyro, Δf repetitively traces the entire response curve for $-\Omega_B \leq \Omega \leq \Omega_B$*

100-square-centimeters, a rotation rate of one degree per hour induces a beat frequency of about one hertz. In practice the laser gyro often is operated in an integrating mode, in which each cycle of the difference-frequency signal is counted as a unit of angular displacement; the correspondence generally is on the order of arcseconds per pulse, and is specified as the scale factor.

Lock-in effects at low angular rates

Early investigations revealed that the linear relationship of Eq. 1 was not obeyed at low rotation rates, where the difference frequency remained locked to zero. The frequency-synchronization effect or frequency "lock-in" is a consequence of a minute amount of coupling due to backscattering between the two travelingwave oscillations. As a result the difference frequency Δf obeys

$$\Delta f = \begin{cases} 0 & \text{for } \Omega^2 \leq \Omega_c^2 \\ \dfrac{4A}{\lambda p}\sqrt{\Omega^2 - \Omega_c^2} & \text{for } \Omega^2 > \Omega_c^2 \end{cases} \qquad (2)$$

and approaches the ideal linear behavior of Eq. 1 only in the limit of high angular rates, as shown in Fig. 2. The critical or lock-in rate Ω_c defines the deadband: $-\Omega_c \leq \Omega \leq \Omega_c$. Typcially Ω_c assumes values on the order of hundreds of degrees per hour. Although the lock-in rate can be minimized by paying careful attention to optical-surface quality, the mere presence of the gain medium in the cavity suggests that lock-in effects never can be entirely eliminated.

The lock-in problem has been the major source of frustration in the 14-year history of laser-gyro development. The usual solution is to impose a bias, which is an artificial optical path-length difference between oppositely directed traveling waves that induces a frequency split (bias frequency) even in the absence of the rotational motion that the instru-

ment is designed to sense or measure. A bias thus is equivalent to a controlled rotational input that shifts the operating range away from the lock-in zone. Only two biasing methods have been seriously pursued thus far, one relying on rotational effects (the "mechanical-dither" technique), and the other on nonreciprocal magneto-optic effects (faraday cells, magnetic mirrors, or differential laser gyros).

Mechanical dither yields best results

Inertial-grade accuracy has been obtained only by Honeywell Inc.[4] employing a mechanical bias — or dither — applied in the form of a periodically reversed rotational motion of small amplitude. The choice of an internal mirror or integral design reflects the philosophy of minimizing the number of internal optical surfaces, and hence the lock-in rate. To implement such a system, however, it was necessary to address several subsidiary problems, including lifetime, and the surface quality of mirrors directly exposed to a plasma. In the Honeywell system, the gain medium occupies the entire optical path of the ring cavity, which is drilled out of a monolithic block of a special low-temperature-coefficient ceramic material, typically Cervit. The construction of such a laser gyro is a delicate affair, requiring time-consuming manual assembly, alignment and testing in ultra-clean environments, procedures that are reminiscent of mechanical-gyro technology, and that contribute significantly to cost. Honeywell is now seeking to develop procedures that will simplify these tasks and thus reduce costs.

Less success with magneto-optic biasing

Magneto-optic techniques have the virtue of preserving the purely nonmechanical nature of the instrument, and typically they are implemented with a modular plasma-tube design. The basis of these techniques is the dependence of the refractive index of a magneto-optic medium on the direction of wave propagation (nonrecipriocity). Magnetic effects of this kind also are familiar in such nonreciprocal microwave devices as the gyrator and circulator.

Of the two magneto-optic effects that have been applied to ring-laser biasing, the more familiar is the faraday effect. Biasing is achieved with an intracavity magneto-optic element surrounded by a current-carrying solenoid and situated between two orthogonally-aligned quarterwave plates. The problems with the faraday-cell technique arise from the difficulty in stabilizing the bias frequency, which depends on several factors including the solenoid current, the temperature of the magneto-optic element, and the presence of stray magnetic fields. Furthermore the presence of the additional optical surfaces of the faraday cell causes an undesirable increase in the lock-in threshold rate.

Bias stability is critical because there is no way to distinguish a shift in the bias from a true rotation. To achieve the requisite stability, an alternating rather than a fixed bias typically is applied, so within each bias period drift errors occur with approximately equal magnitude, but opposite sign. (The mechanical-dither technique illustrates the same principle.) This advantage is offset partially by the fact that the instrument passes through the dead zone twice during each bias cycle. In addition, the periodic waveform driving the bias must be perfectly symmetric, because departures from symmetry are equivalent to a constant effective drift rate. A further difficulty occurs for rotation rates comparable with the magnitude of the periodic bias, since an unduly large time is then spent in the dead zone; to avoid this some systems employ an alternating bias at low angular rates and a fixed bias at higher rates.

Despite the most careful attempts to implement the faraday-cell technique, with an alternating bias, and with stringent current and temperature controls and elaborate shielding against stray magnetic fields, success has remained elusive, and this approach has been all but abandoned. Two alternative magneto-optic techniques have been pursued that appear to be greatly superior to the simple faraday-cell approach.

Magneto-optic alternatives

One relies on the kerr magneto-optic effect, in which nonreciprocal phase shift is imparted upon reflection rather than in transmission as in the faraday effect. Pioneered by the Sperry-Rand Corp.[4] and known as the "magnetic-mirror" technique, this approach incorporates a mirror with a magnetized surface. The improvement over the faraday cell is due to the fact only a small volume close to the mirror surface is sensitive to magnetic fields. Typically the sign of the bias is sequentially reversed.

In a third magneto-optic technique, the basic nonreciprocity is derived from a faraday element, but improved performance is obtained with two traveling waves of orthogonal polarization propagating in each direction. By suitable disposition of the four oscillation frequencies, two difference frequencies can be detected having a common variation due to faraday bias drifts, but the difference-frequency variations with rotation are of opposite sign. With this configuration, called a "differential laser gyro,"[4] subtraction of the two output-signal frequencies yields rotational information that is relatively insensitive to bias drifts.

For any bias technique, large bias magnitude is desirable to achieve isolation from the dead zone and to minimize errors due to the associated nonlinearities. As a practical matter bias magnitude is limited to a value that can be suitably stabilized, by control of the bias parameters (rotational or magneto-optic) mentioned above. Because of the dispersion properties of the gain medium it also is necessary to stabilize the total discharge current and, most importantly, the total optical-path length around the ring. The path-length consideration is one reason for using a housing material with an extremely low temperature coefficient of expansion. Frequently temperature control also is applied to the entire unit.

Most discussions of bias techniques are confined to the patent literature. There are well over one hundred laser-gyro patents, and almost all are directed to the lock-in problem; a large fraction

of the proposed solutions are variations on the magneto-optic theme. These and other aspects of laser-gyro design have been discussed in a few technical reviews.[5]

Errors from gas-flow effects

Problems other than lock-in also have been addressed. One of particular importance is control of the langmuir-flow bias, which is associated with gas-flow effects in a plasma discharge[6] and which produces a difference frequency not related to rotational motion. Such errors can be reduced with a split discharge design, employing a double anode with a common cathode, and stabilizing the differential discharge current.

In specifying laser-gyro performance, it also is important to consider the behavior of the scale factor. As is evident from Eq. 2, the scale factor depends not only on the cavity dimensions and the wavelength of operation, but also varies with rotation rate and lock-in rate in the nonlinear region of the response curve. In general there appears to be a correlation between good bias stability and good scale-factor stability, although this need not always be the case.

It is evident that considerable care and skill are required to make a ring-laser oscillator into a reliable rotation sensor. For this reason attention again has turned to passive rotation sensors, which do not exhibit lock-in or langmuir flow problems because they do not contain an internal active-gain medium. In these methods an optical-sensor circuit is interrogated by laser radiation that is generated externally. These devices, which have equal claim to be called "laser gyroscopes," are more sophisticated and sensitive than the simple sagnac interferometer. In one case sensitivity is improved by means of a fiber-optic ring circuit providing a long optical path.[7] Another approach is to detect the rotationally-induced differential shift in resonant frequency for the two directions of propagation in a passive ring cavity.[8]

In summary, it is clear that the laser gyro offers unique capabilities not otherwise available. Although simple in concept, the device exhibits complexities of behavior that must be thoroughly understood before high accuracy can be realized in a cost-effective manner. In time, however, the laser gyro will take its place as a reliable and accurate rotation sensor that will provide important design flexibility for the avionic systems of the future.

References

1. For a review of the sagnac effect see E. J. Post *Rev Mod Phys 39* 475 (1967)
2. A. A. Michelson and H. G. Gale *Astrophys J 61* 137 (1925)
3. A. H. Rosenthal *J Opt Soc Am 52* 1143 (1962)
4. Various companies' efforts are described from time to time in *Aviation Week & Space Technology*, most recently Jul 25, 1977 [p44]. Earlier articles appeared in the Nov 24, 1975[p46] and Jan 13, 1975[p48] issues
5. F. Aronowitz, in *Laser Applications Vol. 1* (Academic Press, New York, 1971) p133; J. Killpatrick *IEEE Spectrum 4* 10, 44 (Oct 1967)
6. T. J. Podgorski and F. Aronowitz *IEEE J Quant Electron QE-4* 11 (1968)
7. Victor Vali and R. W. Shorthill *Appl Opt 15* 1099 (1976)
8. Shaoul Ezekiel and S. R. Balsamo *Appl Phys Lett 30* 478 (1977)

RAPID COMMUNICATIONS

This section was established to reduce the lead time for the publication of Letters containing new, significant material in rapidly advancing areas of optics judged compelling in their timeliness. The author of such a Letter should have his manuscript reviewed by an OSA Fellow who has similar technical interests and is not a member of the author's institution. The Letter should then be submitted to the Editor, accompanied by a letter of endorsement from the OSA Fellow (who in effect has served as the referee and whose sponsorship will be so indicated in the published Letter) and a commitment from the author's institution to pay the publication charges. The Letter will be published without further refereeing. The latest Directory of OSA Members, including Fellows, was published as Part 2 of the August 1969 issue of the Journal of the Optical Society of America.

Fiber ring interferometer

V. Vali and R. W. Shorthill

University of Utah Research Institute, Salt Lake City, Utah 84108.

Received 17 February 1976.

Sponsored by Lewis Larmore, U.S. Office of Naval Research.

The sensitivity of a ring interferometer as a rotation detector (gyroscope) can be increased considerably by making the counter rotating beams travel around an area many times. (This is not true for a ring laser.) When the ring interferometer is rotating with an angular velocity ω the observed fringe shift is[1-3] $\Delta Z = (4\omega NA)/\lambda c$, where N is the number of round trips the counter rotating beams make around an area A, λ is the free space wavelength, and c is the free space velocity of light. Such an optical gyroscope would be undesirably large if the area A is made bigger than a few hundred cm^2, or if an air (or vacuum) path is used and N is made larger than 100.

An optical fiber waveguide would keep the size of such an instrument quite small even for $N = 10^4$ or larger. The enclosed area A is made circular in this case, $A = \pi R^2$, where R is the radius of the circle. The fringe shift is

$$\Delta Z = \frac{4\omega N\pi R^2}{\lambda c} = \frac{2\omega LR}{\lambda c}, \tag{1}$$

where L is the length of the fiber used.

To find the optimum length of the fiber to be used in such a gyroscope one considers the photon noise limit. The minimum distance change that can be detected with an interferometer is[4]

$$\Delta X = \left(\frac{\lambda}{2\pi}\right)(B)^{1/2}\left(\frac{h\nu}{\eta P}\right)^{1/2},$$

where B is the bandwidth of the detector, $h\nu$ is the energy per photon, η is the quantum efficiency of the photodetector, and P is the beam power. Therefore, the fringe shift corresponding to the photon noise (the minimum detectable fringe shift) is

$$\Delta Z_n = \frac{\Delta X}{\lambda} = \frac{(B)^{1/2}}{2\pi}\left(\frac{h\nu}{\eta P}\right)^{1/2}. \tag{2}$$

In an attenuating fiber the beam power is given by

$$P = P_0 10^{-\alpha L}, \tag{3}$$

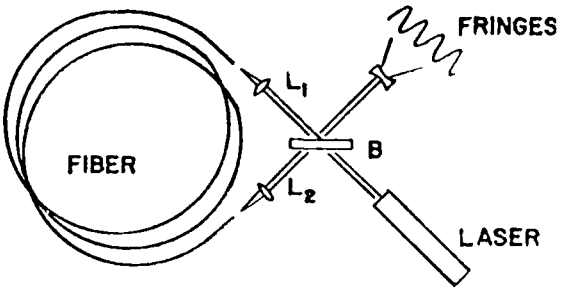

Fig. 1. Experimental configuration of the optical components: L_1 and L_2 are the converging lenses, and B is the beam splitter.

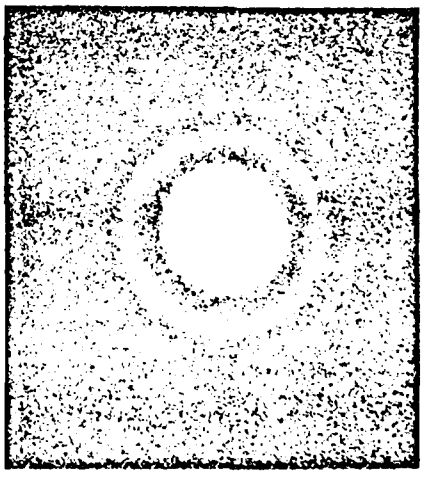

Fig. 2. The observed fringe pattern. High contrast was obtained by equalizing the spatial intensity distributions of both beams.

where P_0 is the initial laser power and α is the attenuation coefficient (given usually in dB/km). By maximizing the SNR with respect to the fiber length L [Eqs. (1), (2), and (3)] one gets for the optimum $L = 0.87(1/\alpha)$. For a 2-dB/km fiber $L = 4.3$ km. Using a 3-mW laser as the light source the minimum detectable rotation rate is (for $R = 15$ cm, $\alpha = 2$ dB/km, $B = 10\ \text{sec}^{-1}$, and $\eta = 0.5$):

$$\omega_{\min} \simeq 1.5 \times 10^{-9}\ \text{rad/sec}$$

These considerations indicate that a sensitive ring interferometer gyroscope can be built if the optical fiber waveguide retains a well defined wavefront and if the coupling efficiency of light into the fiber is not too small. A ring interferometer was therefore built using a single mode fiber (Fig. 1). The laser light, divided by a beam splitter, was focused on the fiber ends. After traversing the fiber and exiting, the single fiber mode is made into a parallel beam again by the other lens that also serves as the focusing lens for the beam traversing the fiber in the opposite direction. Both beams are recombined at the beam splitter. The resultant image is magnified and displayed on a screen. It is seen that both beam pathlengths are identical. Therefore, by moving one fiber end axially one changes the optical pathlength of both (counterrotating) beams by identical amounts. Nothing is therefore changed for the center of the spherical wavefronts that emerge from the fiber ends. Both beams see identical optical pathlengths regardless of the adjustment; on the optical axis the fringe stays bright. The relative divergence can be changed, however, by moving one end of the fiber slightly away from the focal point of the lens. This displaces the center of one spherical wavefront (the end of the fiber) with respect to the other. The result is the experimentally obtained circular fringe pattern shown in Fig. 2. It is important to note that when the distance from the lens to the fiber end on one side is decreased and the fringes grow smaller, the decrease of the corresponding distance on the other side of the interferometer should increase the fringe size. This was observed and used as one criterion for deciding that the fringes are indeed formed by the beams that traversed the fiber.

In obtaining the fringe pattern an over-all efficiency of about 25% was obtained: one quarter of the light emitted by the laser (Spectra-Physics model 138) was used to form the fringes. In spite of using uncoated optics the stray reflections from the lenses and the fiber ends were comparatively weak and were hardly observable. The efficiency of coupling light into the fiber was about 50%. The single mode fiber used in these experiments was 10 m long and was wound on a cylinder 15 cm (6 in.) in diameter. Its core diameter is about 11 μm, and the attenuation for $\lambda = 6328$ Å is about 15 dB/km. It was made by the Corning Glass Works.

These experiments show that a ring interferometer gyroscope having sufficient sensitivity for navigation can be built. Comparing the ultimate theoretical sensitivities the ring laser is still better, but the ring interferometer has the considerable advantage in that it has no effect corresponding to pulling and lockin[5] and can therefore be used to detect very low angular velocities.

This work was funded in part by NSF grant DES 75-120.

References

1. G. Joos, *Theoretical Physics* (Hafner, New York, 1950), p. 471.
2. E. J. Post, Rev. Mod. Phys. 39, 475 (1967).
3. S. Balsamo, S. Ezekiel, and V. Vali, Laser Focus 11, 8 (1975).
4. G. E. Moss, L. R. Miller, and R. L. Forward, Appl. Opt. 10, 2495 (1971).
5. J. Kilpatrick, IEEE Spectrum, 44 (October 1967).

Electromagnetic radiation, relativity, and anomalous red-shifts

Ernest W. Silvertooth

974 Flintridge Avenue, Pasadena, California 91103.
Received 23 May 1975; revised manuscript received 19 January 1976.
Sponsored by John Strong, University of Massachusetts.

The Lorentz transforms and the two postulates are the essence of special relativity. In what follows let us accept the validity of the Lorentz transforms and show, based on an observability assumption, that the two postulates are mutually inconsistent.

Consider a line segment L in an unprimed frame, along which a wave is progressing. The total phase change in the wave is the product of the transit time and the frequency, or $\delta = L\nu/c$. Likewise, in a primed frame the corresponding phase change is $\delta' = (L'\nu')/c'$.

Invoking the Lorentz transforms,

$$L' = \frac{L}{\gamma},\ \nu' = \nu/\gamma \qquad (\bar{v}, L \text{ collinear}),$$

or

$$\delta' = \frac{L\nu}{c'\gamma^2}$$

and

$$\delta' - \delta = L\nu\left(\frac{1}{c} - \frac{1}{c'\gamma^2}\right).$$

If the δs are observables, the assumption, then, by the first postulate $\delta' - \delta = 0$, or $c' \neq c$, which is in violation of the second postulate. Conversely, accepting the second postulate, $c' = c$, then $\delta' - \delta \neq 0$.

Let us now turn to the experiment of Sagnac to justify the assumption. A description of the Sagnac interferometer may be found in a paper by Post.[1] In essence, light from a source is split into two counterdirectional beams, which after traversing the perimeter of a common area A are recombined to produce a fringe pattern. When the interferometer is rotated at an angular velocity $\bar{\theta}$, the fringes are observed to shift in phase an amount $\delta = 4\bar{\theta}\cdot\bar{A}/c\lambda$, the scalar product denoting proportionality of δ to the cosine of the angle between the axis of rotation and the normal to the plane of the optical paths.

Further, it may be shown that δ is independent of the shape of A, or the coordinates of the center of rotation. One may thus invoke paths of particular shape and locate the axis of rotation at will. Consider an interferometer as shown in Fig. 1. The center of rotation is located at o. The two paths are ab and aob, with $ao = ob = r$, and $ab = L$. The phase shift along any line element ds is

$$d\delta = \bar{v}\cdot\frac{ds}{c\lambda}$$

Since the velocity vector $\bar{v}$ in this interferometer is normal to the paths ao and bo, the phase shifts in these two paths are zero. In any event, in the case of rotation they

See Also AIAA J. Oct 73, P1384

APPENDIX E

Er^{3+} $^4S_{3/2}$ nonradiative decays [C.B. Layne and M.J. Weber (unpublished)] and from time-resolved $^2E \rightarrow {}^4A_2$ fluorescence spectra and decays of Mo^{3+} [M.J. Weber and A.J. DeGroot (unpublished)].

[11]W.F. Krupke, IEEE J. Quantum Electron. QE-10, 450 (1974).
[12]C.B. Layne and M.J. Weber (unpublished).
[13]T. Kushida and E. Takushi, Phys. Rev. B 12, 824 (1975).

Passive ring resonator laser gyroscope*

S. Ezekiel and S. R. Balsamo†

Research Laboratory of Electronics, Massachusetts Institute of Technology, Cambridge, Massachusetts 02139

(Received 24 January 1977; accepted for publication 1 March 1977)

A new method of measuring inertial rotation is presented. It is based on the use of a passive ring resonator as the rotation sensing element and an external laser for measuring the difference between the clockwise and counterclockwise lengths of the resonator. Preliminary performance data is included.

PACS numbers: 06.30.Gv, 42.60.Da, 93.85.+q, 94.80.Vc

The use of lasers in the measurement of inertial rotation has been receiving considerable attention for more than a decade. The major effort has been in the development of a ring laser which supports two counter-propagating oscillators that share a common cavity as well as a common amplifier.[1] In the presence of rotation with respect to inertial space perpendicular to the plane of the cavity, the degeneracy in the frequencies of the two oscillators is removed. This is caused by the fact that the optical length of the clockwise (CW) and counterclockwise (CCW) paths around the ring are no longer equal, as demonstrated by Sagnac.[2]

In this paper we report a new method of measuring inertial rotation, also based on the Sagnac effect, which promises to be free from the major problems normally encountered in the ring laser gyroscope, such as the lock-in phenomenon at low rotation rates, bias drift, and scale factor variation which are all attributable to the presence of the gain medium within the ring cavity.[3]

The new concept is based on the use of a passive ring Fabry-Perot interferometer as the rotation sensing element and the use of an external laser to measure any difference between the CW and CCW lengths of the cavity caused by inertial rotation. Because the reference cavity is passive, all the problems normally associated with the gain medium in the conventional ring laser gyroscope are eliminated.

Several schemes of implementing such a concept are possible but only two are discussed here and are illustrated in Fig. 1. One scheme, shown in Fig. 1(a) employs two independently controlled laser frequencies to measure the CW and CCW resonance frequencies of the passive ring. To avoid the problem of uncorrelated laser jitter when two separate lasers are used, we have chosen to derive the two independently controlled laser frequencies from one laser by the use of two frequency shifters such as acousto-optic devices. As shown in Fig. 1(a) the frequency of an external laser f_0 is shifted to $f_0 + f_1$ by an acousto-optic crystal driven at f_1 and to $f_0 + f_2$ by another crystal driven at f_2. As long as f_1 and f_2 are derived from low jitter rf oscillators, the frequency jitter in $f_0 + f_1$ and in $f_0 + f_2$ are identical. The measurement of cavity path-length difference may be accomplished by locking the CW resonance frequency of the cavity to $f_0 + f_1$ by means of an electronic feedback loop using a piezoelectric length transducer,[4] as shown in Fig. 1(a). A second feedback loop is used to lock $f_0 + f_2$ to the CCW resonance frequency of the cavity by adjusting f_2. In this way, the difference between f_1 and f_2 is directly proportional to inertial rotation.

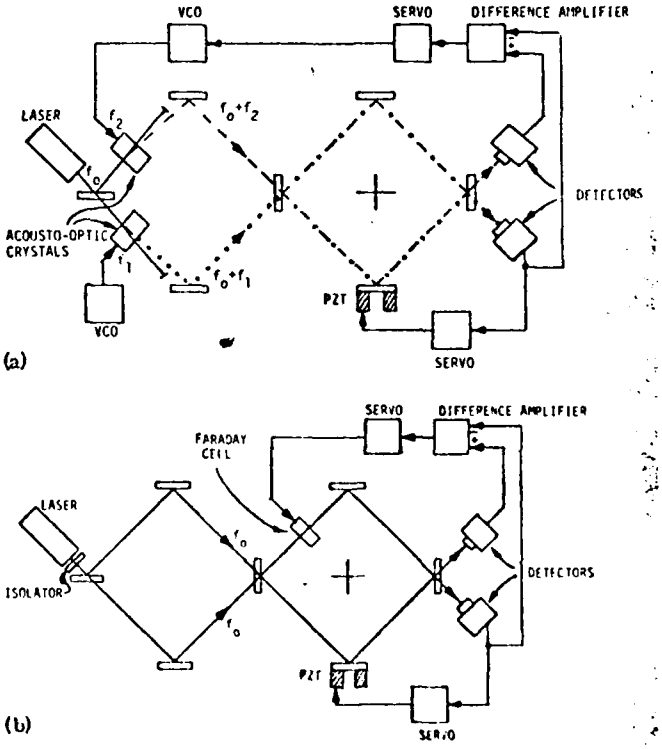

FIG. 1. Schematic diagram of two configurations for a passive ring resonator laser gyroscope. (a) using acousto-optic frequency shifters and (b) using an intracavity Faraday cell.

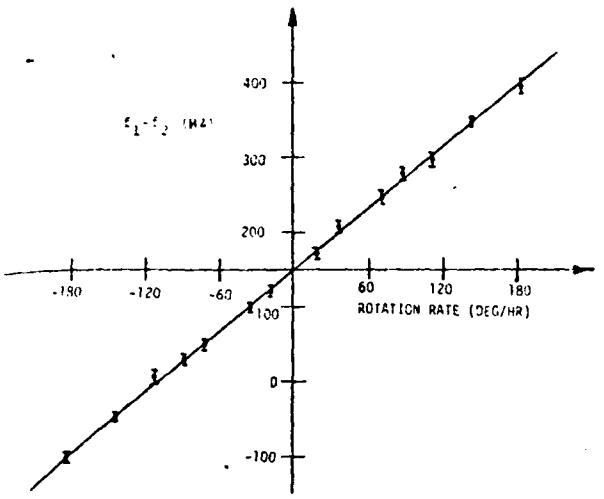

FIG. 2. Measured frequency difference $(f_1 - f_2)$ as a function of rotation rate Ω.

Another scheme, shown in Fig. 1(b) employs only one laser frequency and a means of nulling out any difference between CW and CCW path length caused by inertial rotation by using, for example, a Faraday cell within the cavity. As shown in Fig. 1(b), the CW resonance frequency of the cavity is locked to the laser frequency f_0. In the presence of inertial rotation, the CCW resonance frequency will no longer be at f_0 and this frequency difference is then used as an error signal in a feedback loop driving the Faraday cell to bring the CCW resonance frequency back to f_0. In this way, the current needed to drive the Faraday cell is directly proportional to inertial rotation.

In both schemes, the difference between CW and CCW resonance frequencies of the cavity Δf caused by a rotation Ω normal to the plane of the cavity is given by the Sagnac effect[5] as

$$\Delta f = (4A/\lambda P)\Omega,$$

where A is the area enclosed by the cavity, P is the perimeter, and λ is the wavelength of the light. The precision with which Δf can be measured depends on the Q of the cavity, in other words on the instrumental linewidth of the cavity Δf_c and on the signal-to-noise ratio in the measurement. Assuming shot-noise-limited detection, it should be possible to measure a rotation rate with an uncertainty $\delta\Omega$ given by

$$\delta\Omega \approx 10^5 \lambda P \Delta f_c / 4A(N\eta\tau)^{1/2} \quad \text{deg/h},$$

where N is the number of photons per second transmitted at the peak of the cavity resonance, η is the photodetector quantum efficiency, and τ is the integration time. For example, for $\lambda = 6328$ Å, $P = 40$ cm, $A = 100$ cm^2, $\Delta f_c = 1$ MHz, $N = 2\times10^{11}$ photons/sec, $\eta = 0.5$, and $\tau = 1$ sec, we get $\delta\Omega \approx 0.05$ deg/h.

We have performed preliminary experiments using the configuration in Fig. 1(a). We used a square cavity made of solid aluminum, measuring 17.5 cm on a side. The corners are terminated with two flat and two curved mirrors and one of the cavity mirrors is mounted on a piezoelectric transducer. The output from a linearly polarized 1-mW single-frequency He-Ne laser is split into two beams, each of which is upshifted by an acousto-optic crystal and then coupled into the cavity. The acousto-optic crystals are driven by two stable and independent voltage-controlled oscillators operating around 40 MHz. In our setup, the CW cavity resonance is locked to $f_0 + f_1$ and f_2 is adjusted by a second feedback loop so that $f_0 + f_2$ is held at the resonance frequency of the CCW cavity. To eliminate the effect of cavity and laser jitter on the measurement of f_2, the outputs of the two detectors are subtracted so that only their difference is fed as an error signal into the second feedback loop. In this way, the second loop is only sensitive to a nonreciprocal cavity length change such as that caused by inertial rotation.

The entire setup was placed on a motor driven turntable. Figure 2 is a plot of $f_1 - f_2$ as a function of table rotation rate Ω. The linear relationship between $f_1 - f_2$ and Ω indicates the absence of lock-in between the counterpropagating frequencies. This is as expected since any coupling between the CW and CCW frequencies, for example, by backscattering at mirror surfaces, causes frequency pulling but not lock-in. In our setup, it is easy to measure any coupling between the beams by simply blocking one beam and observing the backscattered light transmitted in the opposite direction. We measured such backscattering and found it negligible.

The bias drift was also investigated. Figure 3 shows $f_1 - f_2$ as a function of time while the turntable was stationary. No noticeable drift was detected in a time interval of 1 h. The rms fluctuation in the output for $\tau = 10$ sec corresponds to about 10 deg/h and this is large compared with anticipated values for the present setup. Several sources of noise are being investigated. A more detailed paper on our experiments will be submitted for publication shortly.[6]

The passive ring resonator methods of measuring inertial rotation discussed in this paper are of course not free of potential problems. The stability of the cavity as well as the stability of the alignment of the

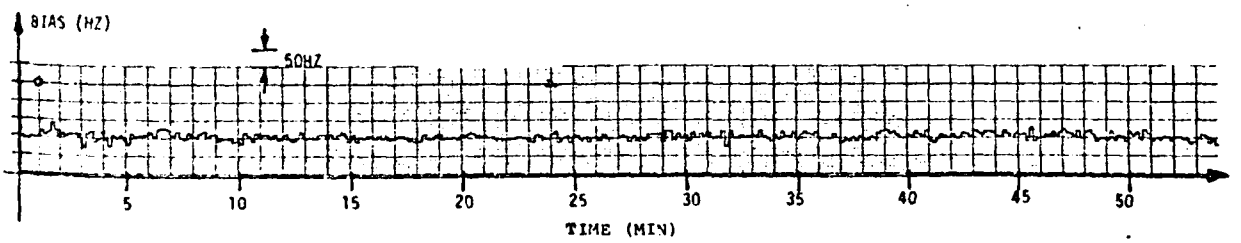

FIG. 3. Measured frequency difference $(f_1 - f_2)$ as a function of time (turntable stationary); integration time = 10 sec. An $f_1 - f_2$ of 50 Hz is equivalent to a rotation rate of 37 deg/h.

external beams are crucial. Considerable care must be exercised to ensure that both cavity directions are excited in the same manner. Errors can also be caused by changes in the polarization of the light, changes in intensity, as well as nonideal performance of the electronic feedback loops.[6] Furthermore, to achieve a constant scale factor ($4A/\lambda P$) the laser frequency must be long-term stabilized, for example, to the center of the gain curve or Lamb dip. The serious problem of the reflected beams reentering the laser is prevented in the configuration of Fig. 1(a) by the presence of the acousto-optic crystals and in Fig. 1(b) by an optical isolator, for example, an acousto-optic crystal.

The concepts outlined in Fig. 1 may be applied to the construction of large-area ring cavities for applications in geophysics such as earth wobble measurements or in testing of precision turntables or gyroscopes. If a ring cavity, 2 m on a side, is used with a 3-W single-frequency argon ion laser, it should be possible to measure earth rotation with an uncertainty of 5 parts in 10^9 in an integration time of 1000 sec.

An exciting possibility is to replace the mirror-terminated cavity with a closed fiberoptic ring.[7] Low-loss single-mode fibers are available so that the only major problem remaining is the design of efficient means of coupling light into and out of the fiber ring. Such possibilities are under investigation in our laboratory including the use of semiconductor and Nd-YAG lasers.

Finally, the highly precise techniques for the measurement of small path length or phase shift in a ring cavity described in this paper are clearly applicable in spectroscopy. For example, if a gas cell is placed within the cavity and an intense beam from a tunable laser is propagated along one direction and the same but much weaker beam is propagated in the opposite direction, it would then be possible to perform saturated dispersion spectroscopy[8] of the gas in the cell. The sensitivity of such a method would be extremely high coupled with the high-resolution capability made possible by the saturation effect. Another spectroscopic application that is being pursued in our laboratory is the use of the concepts in Fig. 1 to detect parity nonconservation due to weak neutral currents by measuring the phase difference between right circularly polarized and left circularly polarized light propagating in opposite directions in a cell (or in an atomic beam) of cesium.[9]

*Supported by the Air Force Office of Scientific Research.
†Major, U.S. Air Force.
[1]W. Macek and D. Davis, Appl. Phys. Lett. 2, 67 (1963).
[2]G. Sagnac, C.R. Acad. Sci. (Paris) 157, 708 (1913); 157, 1410 (1913).
[3]F. Aronowitz, *Laser Applications*, edited by Monte Ross (Academic, New York, 1971), pp. 134—200.
[4]F.Y. Wu, R.E. Grove, and S. Ezekiel, Appl. Phys. Lett. 25, 73 (1974).
[5]A.H. Rosenthal, J. Opt. Soc. Am. 52, 1143 (1962).
[6]S.R. Balsamo and S. Ezekiel (unpublished).
[7]This is not to be confused with the two-beam fiber interferometer proposed by Vali and Shorthill [Appl. Opt. 15, 1099 (1976)].
[8]C. Bordé, G. Camy, B. Decomps, and L. Pottier, Colloq. Int. C.N.R.S. 217, 231 (1974).
[9]C. Bouchiat and M.A. Bouchiat, Phys. Lett. B 48, 111 (1974); J. Phys. (Paris) 35, 899 (1974).

Seventh harmonic conversion of mode-locked laser pulses to 38.0 nm

J. Reintjes, C. Y. She,* R. C. Eckardt, N. E. Karangelen, R. A. Andrews, and R. C. Elton

Naval Research Laboratory, Washington, D. C. 20375
(Received 14 February 1977; accepted for publication 3 March 1977)

Seventh harmonic generation in helium is used to produce coherent light at 38 nm from laser pulses at 266.1 nm. The variation of both the fifth and seventh harmonic signals with helium pressure is described.

PACS numbers: 42.65.Cq

Frequency upconversion using nonlinear optical interactions have proven to be an important source of coherent radiation in the vacuum ultraviolet region of the spectrum.[1,2] We have previously reported[3] the generation of coherent light at 53.2 nm through fifth harmonic conversion of laser pulses at 266.1 nm. In this paper we describe the first observation of seventh harmonic conversion of laser radiation and the generation of coherent light at 38 nm in helium; this is the shortest-wavelength coherent radiation which has yet been reported. In addition to reporting this new wavelength radiation we present measurements of both the fifth and seventh harmonic signals as a function of helium pressure. These results show that conversion efficiency varies as N^2 for low pressures (N = helium density), and shows a weaker dependence for pressures above 10 Torr. Possible sources of this limitation on conversion are discussed.

A partial energy level diagram of helium is shown in Fig. 1 where the levels involved in the harmonic generation processes are indicated. The fifth harmonic

APPENDIX F

STANFORD UNIVERSITY
STANFORD, CALIFORNIA 94305

DEPARTMENT OF MATERIALS SCIENCE AND ENGINEERING

3 March 1978

Dr. William T. Mayo, Jr.
Spectron Development Laboratories, Inc.
3303 Harbor Blvd.
Costa Mesa, California 92626

Dear Dr. Mayo:

I have given some thought to the problem described in your letter of 24 February. It appears to me that adaptation of the passive resonator device proposed by Ezekiel is certainly worthy of your further consideration.

The sensitivity of such a device to fluid flow effects is the same as for an active resonator, and is estimated on the last page of Rosenthal's paper (J. Opt. Soc. Am. 52, 1143, 1962) to be on the order of several kHz per cm/sec longitudinal flow velocity for water. The principal difference between this type of sensor and the active oscillator device is the signal/noise limitation due to resonator linewidth. The information of interest is the flow-induced differential shift in cavity resonant frequencies, but this is generally much less than the width of the cavity resonance. The latter are typically on the order of a few MHz - losses due to absorption and scattering would broaden this somewhat, depending on the length of the sample cell and the properties of the liquid. (It is evident that a long sample cell increases sensitivity, but decreases detectivity, due to increased losses and linewidth; there may be an optimum value). For a 1 cm/sec flow velocity of water the ratio of line shift to linewidth is therefore about 1:1000. This is certainly detectible, although care is required. In fact, rotationally induced shifts substantially below 1 kHz have been detected; see Fig. 2 of the paper by Ezekiel and Balsamo.

I would be greatly concerned however if it were necessary to expose mirror surfaces to a liquid environment. This could create an entirely new set of problems.

To the best of my knowledge ring laser flowmeters have not received a great deal of attention, although I must admit that I do not monitor this application too carefully. There was an article on this subject by Fenster and Kahn in Applied Optics 7, 2383 (1968), and very brief mention of a Sperry device was made in an obscure journal called Canadian Chemical Processing (November 1969, p. 65). The latter article claims that "Laser flowmeters have been built for hydrazine, nitrogen tetroxide, and natural gas. Water and Freon have also been measured regularly". The reference of course is to an oscillator-type device. (If you want to track down more recent articles, you might search the Science Citation Index for the Fenster and Kahn reference).

I hope these brief remarks will be of some help to you.

Very truly yours,

Howard Greenstein

Howard Greenstein

APPENDIX G

TO: DR. P. SELWYN (ARPA TTO)

FM: W. STACHNIK (NUSC NL)

Telecopy to P. Selwyn
April 7, 1978

SUBJECT : OPTICAL VORTICITY METER

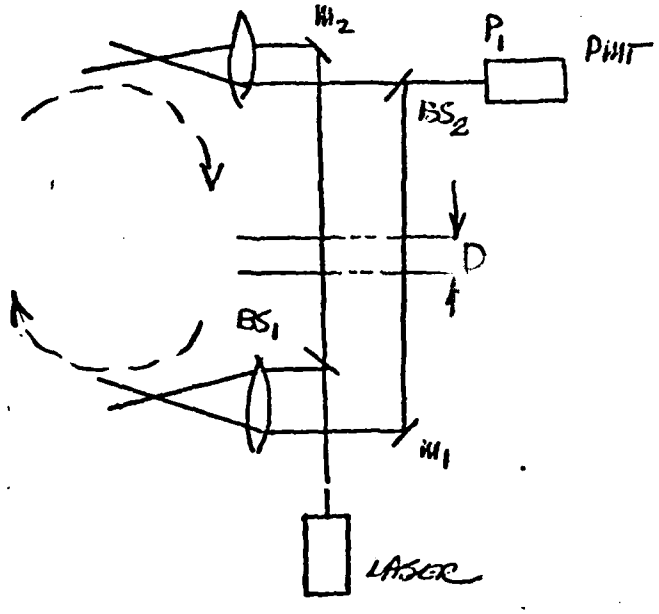

(1) THE ABOVE CONFIGURATION IS AN OPTICAL-PATH-BALANCED HOMODYNE VELOCIMETER. THE UNIQUE ASPECT OF THE CONFIGURATION INVOLVES THE COMBINATION OF TWO SCATTERED WAVE FRONTS ON P_1, THE SYSTEM'S DETECTOR. IN THIS CONFIGURATION A 10^{-3} m/sec FLOW CIRCULATION WILL PRODUCE A 600Hz SHIFT FROM ZERO FREQUENCY. AT 1 m/sec THE SHIFT WOULD BE 600 KHz.

(2) BECAUSE OPTICAL PATHS ARE BALANCED, "D" CAN BE ADJUSTED TO MATCH "S", THE SAME SIZE OF THE DISTURBANCE (IF PRACTICAL)

(3) THE SENSE OF THE CIRCULATION CAN NOT BE DETERMINED IN THE PREVIOUS CONFIGURATION. THIS HOWEVER CAN BE CORRECTED WITH THE CIRCUIT ADDITIONS SHOWN DOTTED IN THE NEXT DIAGRAM.

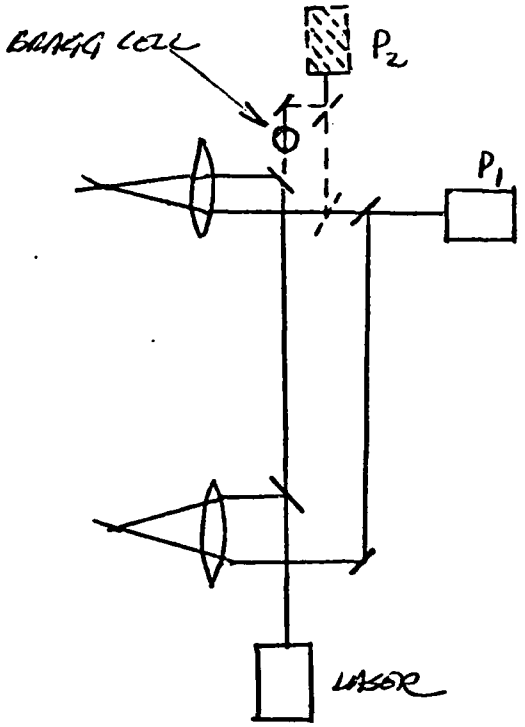

THE ADDITION IS THAT OF A SECOND PHOTOMULTIPLEXER AND BRAGG CELL IN ONE LEG OF THE HOMODYNE SYSTEM. THE BRAGG CELL WILL PREVENT ZERO FREQUENCY OUTPUT AND THEREFORE MAINTAIN THE SENSE OF THE VELOCITY IN THE UPPER PROBE VOLUME.

AREAS REQUIRING ANALYSIS ARE:

A. HOMODYNE EFFICIENCY RELATED TO THE RANDOM PHASE OF THE TWO SCATTERED WAVEFRONTS

B. TRANSIT TIME BROADENING

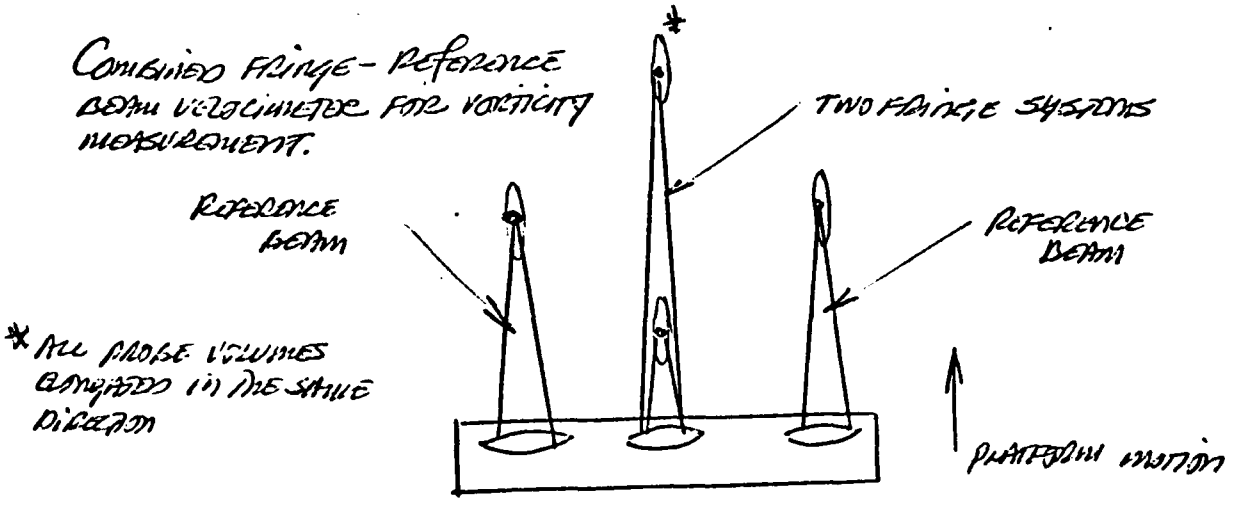

MIAGO HAS ALSO SUGGESTED A MULTIPLE CONFIGURATION WHICH MAY BE LIKE THE ABOVE. FERNANDER HAS SUGGESTED A DISPERSED BACKSCATTER APPROACH WHICH IS VERY INTERESTING BECAUSE IT CONFORMS MOST TO THE DEFINITION $\frac{\oint \vec{v} \cdot d\vec{c}}{A}$